Fiducial Reference Measurements for Satellite Ocean Colour Phase-2

TR: *Harmonised cal/char lab guidelines, including lab protocols for FRMOCnet OCR models*

(FRM4SOC2-TR D12)

Title	TR: Harmonised cal/char lab guidelines, including lab protocols for FRMOCnet OCR models
Document reference	FRM4SOC2-D12
Project	EUMETSAT – FRM4SOC Phase-2
Contract	EUMETSAT Contract No. EUM/CO/21/460002539/JIG
Deliverable	TR D12
Version	v.4.3
Date issued	15.01.2026

Prepared By	Approved by
Name: Viktor Vabson	Name: Juan Ignacio Gossn
Organisation: UT	Organisation: EUMETSAT
Position: Task 6 Leader	Position:
Date: 15.01.2026	Date:
Signature:	Signature:

Funded by the European Union

Fiducial Reference Measurements for Satellite Ocean Colour Phase-2

TR: *Harmonised cal/char lab guidelines, including lab protocols for FRMOCnet OCR models*

(FRM4SOC2-D12)

TECHNICAL REPORT

Viktor Vabson, Ilmar Ansko, Riho Vendt, Joel Kuusk

UNIVERSITY OF TARTU
Tartu Observatory
1632

2026

PROGRAMME OF THE EUROPEAN UNION
Copernicus Europe's eyes on Earth
IMPLEMENTED BY EUMETSAT

Document Control Table

Title	TR: Harmonised cal/char lab guidelines, including lab protocols for FRMOCnet OCR models
Document reference	FRM4SOC2-D12
Project	EUMETSAT – FRM4SOC Phase-2
Contract	EUMETSAT Contract No. EUM/CO/21/460002539/JIG
Deliverable	TR D12
Version	v.4.3
Date Issued	15.01.2026

Document Change Record

Index	Issue	Revision	Date	Brief description	Issued by
1	1	0	12.04.2022	Original issue	V. Vabson
2	2	0	21.07.2022	Ver.2. Updates after EUMETSAT review	V. Vabson
3	2	1	27.09.2022	Ver.2.1. Updates after NPL review	V. Vabson
4	2	2	10.01.2023	Ver.2.2. Updates after the project workshop	V. Vabson
5	3	0	10.02.2023	Ver.3. Updates after the PM7	V. Vabson
6	3	1	17.06.2024	Ver.3.1 Update with conclusions from LCE (D-13)	V. Vabson
7	4	0	30.09.2025	Update with conclusions from LCE and Uncertainty workshop	V. Vabson
8	4	1	10.10.2025	Update after consortium review	V. Vabson
9	4	2	28.11.2025	Update after CM EUMETSAT review	V. Vabson
10	4	3	15.01.2026	Public release	V. Vabson

Distribution List

Public at https://frm4soc2.eumetsat.int

Contents

Acronyms and Abbreviations

Acronym	Description
AAOT	Acqua Alta Oceanographic Tower
AERONET-OC	The Ocean Colour component of the Aerosol Robotic Network
AMT	Atlantic Meridional Transect
BRDF	Bidirectional reflectance distribution function
Cal	Calibration
CCPR	Consultative Committee for Photometry and Radiometry
CEOS	Committee on Earth Observation Satellites
Char	Characterisation
CIPM	Comité International des Poids et Mesures (International Committee for Weights and Measures)
CIPM MRA	CIPM Mutual Recognition Arrangement
CWL	Central wavelength
EO	Earth Observation
ESA	European Space Agency
EUMETSAT	European Organisation for the Exploitation of Meteorological Satellites
FICE	Fiducial Inter-Comparison Experiment
FidRadDB	”Fiducial Radiometer” Data Base
FOV	Field of view
FRM	Fiducial Reference Measurements
FRMOCnet	Copernicus FRM-certified OC instrument network
FRM4SOC	Fiducial Reference Measurements for Satellite Ocean Colour
FWHM	Full Width at Half Maximum
GEO	Group on Earth Observations
ILAC	International Laboratory Accreditation Cooperation
IOCCG	International Ocean-Colour Coordinating Group
LSF	Line spread function
LUT	Look Up Table
MERIS	Medium Resolution Imaging Spectrometer
MVT	MERIS Validation Team
N/A	Not applicable
NASA	National Aeronautics and Space Administration
NERC	Natural Environment Research Council
NMI	National Metrology Institute
NPL	National Physical Laboratory
OC	Ocean Colour
OCDB	Ocean Colour Database
OCR	Ocean Colour Radiometer
QA	Quality Assurance
QA4EO	Quality Assurance framework for Earth Observation
QC	Quality Control
QTH	Quartz tungsten halogen
PTFE	Polytetrafluoroethylene
ROI	Return On Investment
RSP	Remote Sensing and Products Division
RD	Reference Document
S3	Sentinel-3
S3VT-OC	Sentinel-3 Validation Team – Ocean Colour group
SeaWiFS	Sea-Viewing Wide Field-of-View Sensor

Acronym	Description
SIRREX	SeaWiFS Intercalibration Round Robin Experiments
SI	International System of Units
SLM	Stray light matrix
SNR	Signal to noise ratio
SOW	Statement of Work
SST	Sea Surface Temperature
TO	Tartu Observatory, University of Tartu
TR	Technical Report
UT	University of Tartu
VAL	Validation
VIM	Vocabulaire International de Métrologie (International Vocabulary in Metrology)

1. Scope

The current document describes the harmonised calibration and characterisation (cal/char) guidelines for two ocean colour radiometer types – TriOS RAMSES and Seabird Scientific HyperOCR – to be applied by secondary calibration laboratories. The guidelines establish a shared and common standard at the secondary cal/char laboratory level, ensuring full adoption of traceability requirements for the radiance/irradiance laboratory standards, measurement results and uncertainties. This document forms deliverable TR D12 of the FRM4SOC phase-2 project.

A cal/char lab comparison exercise of hyperspectral instruments has been organised involving multiple actors to verify the performance of SI-traceably calibrated secondary lab standards and apply a protocol for the calibration of their FRM OCR instruments. Formerly published guidelines [1], [2] and results of repeated characterisations and calibrations of two RAMSES and two HyperOCR sensors presented in TR D7 were carefully reviewed and accounted for in preparing the harmonised guidelines document. Differences in hard- and software of OCRs make the characterisation procedure model-dependent and hinder the harmonisation of guidelines. Some new elements in the characterisation procedures for the two most common OCR instrument types - RAMSES and HyperOCR – have been developed to account for the internal heating of radiometers, for the possible asymmetry of angular effects, and to reduce signal hysteresis if used in varying thermal conditions.

The report contains guidelines for secondary laboratory standards, measurement setups for cal/char and traceability requirements for the principal equipment. The next iteration of the current document will include updates suggested during the lab comparison exercise and will be available for the workshop in Task 8 and instrument calibrations before the Acqua Alta Oceanographic Tower (AAOT) field exercise.

The proposed instrument models and types mentioned in this document are just examples for building setups and are not meant as preferred.

2. Introduction

Metrological traceability to the International System of Units [3] is the concept that links all metrological measurements to the SI through a series of calibrations or comparisons. Each step in this traceability chain has a rigorous documented uncertainty analysis. In Metrology the term *comparison* [4] refers the process of validating an uncertainty analysis of measurements obtained from artefacts owned/operated by different laboratories. National Metrology Institutes (NMIs) must participate in regular formal comparisons, usually every ten years, and accredited calibration labs every five years at a suitable technical level. Each technical discipline defines a limited number of "key comparisons", and these provide evidence to support uncertainty analysis of an NMI for a certain number of related quantities in a "Calibration and Measurement Capabilities – CMCs - Database". The Consultative Committee for Photometry and Radiometry (CCPR) has defined a key comparison for six key measurands (spectral irradiance, spectral responsivity, luminous intensity, luminous flux, spectral diffuse transmittance and spectral regular reflectance). Several Round-Robin Experiments arranged during the last decades for testing and validation of performance, calibrations and characterisations of Ocean Colour Radiometer (OCR) instruments demonstrated that firm traceability of measurements to the SI units must exist, and calibration at an NMI or at an accredited laboratory is the preferred option. Spectral responsivity of a radiometer is usually calibrated by measuring a known radiation source aligned at a specified distance. Procedures are well established and validated [1], [5], [6], [7], [8], [9]. Unfortunately, specified and controlled conditions during the calibration in a lab may differ significantly from the conditions that may prevail during later use of the instrument. Examples of these varying conditions are operating temperature, angular variation of the light field (especially for irradiance sensors), the intensity of the measured radiation, spectral variation of the target, etc. Each of these factors may interact with the individual instrument properties when used in the field, and estimation of such uncertainties requires instrument characterisations in addition to the absolute radiometric calibration [2], [10], [11]. Characterisation results describe the properties of individual radiometers. However, the system of two to three radiometers is often used for the determination of remote-sensing reflectance and/or fully normalised water-leaving radiance. Data handling of the three-radiometer system, including uncertainty contributions, is substantially more complicated than the case of a single radiometer. Some parameters, which contribute significantly to the case of a single radiometer, may have almost no effect in a three-radiometer system. For evaluating specific uncertainty contributions to the uncertainty of final products, a particular measurement model and a full set of relevant input quantities must be known. Besides cal/char results, the model's input quantities include additional information, which must be acquired during field

measurements. Therefore, the uncertainty estimates for characterised parameters referred to in this document can only serve as input information for evaluation of contributions in the final products.

Complete cal/char and regular recalibration of OCRs is needed due to significant responsivity drift of sensors, possible bias of single instruments from the ideal realisation of specification values, and for accounting environmental factors, which may affect the results. Therefore, any field radiometer used for the satellite ocean colour validation should have a documented history of SI traceable calibrations and characterisations. Spectral radiometric responsivity should be preferably determined before and after each major field deployment, but at least regularly once a year. Referring to the IOCGG protocols [2] and to the the strategy plan [12], where rather detailed guidelines are given, the general scheme for the complete cal/char presented in these guidelines is in close agreement with previous documents. However, some new approaches used for characterisation of the two most common OCR instrument types - RAMSES and HyperOCR - are summarised in the next paragraphs.

An important finding is that the internal thermal properties of the radiometers may significantly affect cal/char results. Both the dark signal and the radiometric responsivity have significant dependence on temperature, especially above 20 °C and with long (>1 s) integration times. Change of the radiometric response due to the self-heating in stable lab conditions can distort the calibration and characterisation results as small deviations in spectra due to polarization and/or angular effects can be of the same magnitude as the responsivity change of the radiometer. The radiometer's response will drift with the varying internal temperature as a function of the mode of data acquisition process. Internal temperature can rise, but it can also drop if the previous operation mode of the radiometer caused stronger self-heating. To reduce the drift effect due to internal self-heating, the characterization measurement sequence shall include recording a specified reference signal as often as possible. For example, every second measurement shall be the reference measurement (e.g. initial position of the polarizer or initial angle θ=0° in the case of angular measurements).

A rather strong hysteresis of the optical signal of radiometers is evident if the ambient temperature is swept from 5 °C up to 40 °C and back down to 5 °C, and the signal is presented as a function of environmental temperature (*Figure 2-1*). In *Figure 2-1*, the ambient temperature of the radiometer immersed into a water thermal bath is the temperature of water, which can be easily measured with uncertainty below 0.1 °C. The internal temperature of the radiometer is measured with the internal temperature sensor (HyperOCR). Large hysteresis of the optical signal determined with increasing and decreasing temperature cycle implies a significant increase in uncertainty. Hysteresis becomes significantly smaller if the same signal is presented as a function of temperature measured with the internal temperature sensor of the radiometer. This clearly shows the importance of an internal temperature sensor of a radiometer used under variable environmental conditions. In addition, correcting for temperature effects is inefficient without an internal temperature sensor due to the large uncertainty of the determined temperature difference under calibration and use in field. The smallest hysteresis is evident for the signal presented as a function of temperature calculated from the dark signal of the optical sensor. Small hysteresis of the dark signal shown against the internal temperature sensor indicates a good thermal coupling between the internal temperature sensor and the optical detector. This is the best quality indicator showing successful location of the internal temperature sensor. Even though using the dark signal to infer the temperature of an optical sensor will reduce the hysteresis of the optical signal substantially in comparison to using external temperature, this does not spare the need of an internal temperature sensor, as the reliability of this inference without an internal reference sensor is limited.

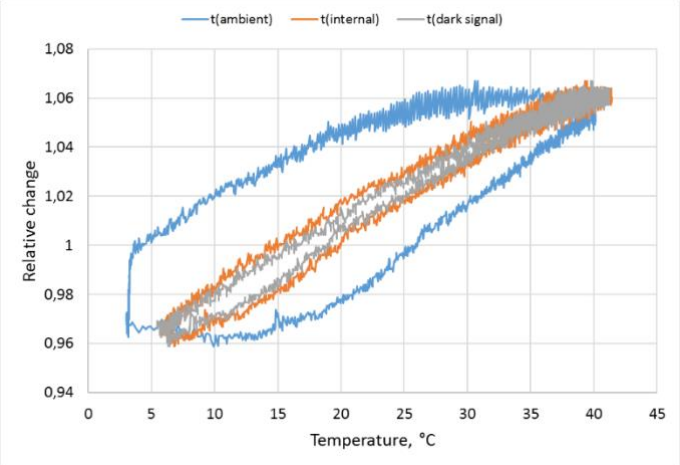

Figure 2-1. The relative change of the radiometer's signal at 850 nm as a function of temperature measured with three different temperature sensors. The reduced hysteresis pattern for the case of internal temperature (orange) shows the relevance of an OCR having an internal thermistor.

Here, both the lab characterisation and later field use should be considered: (1) Dark signal can be used as temperature reference *only* after characterisation in suitable temperature range in comparison with a SI traceable reference thermometer; (2) During field deployment, darks should be regularly measured with the longest integration time, and during the dark measurement the entrance optics shall be occulted via a shutter or a cap. The temperature of the optical sensor during field deployment can be derived if both components of such additional information are available.

Angle characteristics of TriOS RAMSES irradiance sensors are often strongly non-symmetrical and thus, depend on the azimuth angle used for measurements. This circumstance also makes the further use of characterisation results much more difficult: azimuth angle must be specified during characterisation and specified and accounted for during use in the field.

In this document, we present harmonised cal/char lab guidelines, including lab protocols for a calibration and characterisation of the two most common hyperspectral OCR instrument types: RAMSES and HyperOCR, as well as the DALEC OCR, progressively acquiring relevance among the OC community. The general description of the instruments subject to cal/char is given in Section 4. Requirements for laboratories are presented in Section 5. General requirements for cal/char measurements of OCR instruments are presented in Section 6. Description of calibration methods are given in Section 7. Description of characterisation methods following substantially the IOCGG protocols [2] are given in Section 8. Gaps in cal/char protocols of FRM OCR are presented in section 9, re-characterisation routine in section 10, and conclusions in Section 11. Suggested cal/char data formats and necessary auxiliary data formats compatible with the community processor are given in Annex A.

3. Description of the three most common models subject to calibration and characterisation

Differences in hard- and software of OCRs make the characterisation procedure model-dependent and hinder harmonisation of guidelines. In addition, the list of specific parameters to be characterised depends on the selected instrument model. Therefore, attention is focused on the three typical hyperspectral models used for FRM: TriOS RAMSES and Sea-Bird's HyperOCR (both radiance and irradiance sensors, each conforming an independent unit) and *In-situ* Marine Optics DALEC (each unit consisting of an integrated set of two radiance and one irradiance sensor) (Table 3-1, *Figure 3-1*, *Figure 3-2*). The specifications are based on information supplied by the manufacturers of the OCRs [13], [14], [15], of the embedded module MMS 1 [16], and on the results of instrument on-site tests.

Table 3-1. Key parameters of the radiometers.

Parameter	Unit	RAMSES		HyperOCR		DALEC	
		irradiance	radiance	irradiance	radiance	irradiance	radiance
weight	kg	0.9		1.1	0.95	5	
length*	mm	295	395	358	319	210	
diameter	mm	48		60(70)	60	140	
supply voltage	V	12**		9...18		12...24	
average power consumption	W	0.85		4		TBD	
temperature range	°C	+2...+40		-10...+50		0...+50	
temperature control		without temperature stabilisation					
field of view	°	180	7	180	6	180	5
input aperture diameter	mm	7	15	21	20	10	10
wavelength range	nm	350...1000		305...900		305...950	
Si photodiode array	-	CMOS logic compatible					
active area	-	pixel pitch: 25 µm; height: 2.5 mm					
pixel count	-	256					
wavelength step	nm	3.3					
spectral bandwidth	nm	9.5					
integration time	ms	4...8192				1...6000***	
minimum sampling interval	s	1		0.25		0.025	
bits per sample	-	16					
responsivity @ 500 nm & 1 ms	µW^{-1}m^{2}nm	0.6	N/A	0.7	N/A	TBD	N/A
responsivity @ 500 nm & 1 ms	µW^{-1}m^{2}nmsr	N/A	0.1	N/A	0.02	N/A	TBD
internal shutter	-	no	no	yes	yes	no	
internal temperature sensor	-	no	no	yes	yes	yes	

*Cable adds 70 mm.
Different data for physical height of the HyperOCR sensors is provided on the home-page:
https://www.seabird.com/hyperocr-radiometer/product-details?id=60762467730,
https://www.seabird.com/hyperocr-radiometer/product-downloads?id=60762467730
**when using the provided cable
*** from the datasheet

The radiometers are based on the Zeiss MMS1 spectrometer modules, proprietary front-end and data acquisition electronics, RAMSES and HyperOCR are in the watertight housings of cylindrical symmetry, with the optical input and signal connector at the opposite ends of the cylinder. The housing is fabricated from stainless steel (RAMSES) or white plastic (HyperOCR). The optical axis is expected to coincide with the centre of the cylinder. DALEC is a radiometric system designed for the in-air use, it contains three spectrometer modules with pre-aligned input

optics in common case. The wavelength scale, dark signal parameters, temperature coefficients (HyperOCR, DALEC) and radiometric non-linearity coefficients (DALEC) are defined in the calibration files provided by the manufacturer.

Figure 3-1. The radiometers in the focus of the document. 1 - the case, 2 - Sea-Bird's HyperOCR radiance sensor, 3 - HyperOCR irradiance sensor, 4 - TriOS RAMSES radiance sensor, 5 - RAMSES irradiance sensor, 6 - HyperOCR connection harness, 7 - RAMSES connection harness, 8 - alignment jig, 9 - bubble level.

Figure 3-2. The radiometer in the focus of the document: In-situ Marine Optics DALEC.

4. Requirements for laboratories

A secondary laboratory performing calibration and characterisation of OCR instruments for FRM quality measurements [17] shall be able to provide an accreditation certificate to ISO 17025 standard [18] compliant to International Laboratory Accreditation Cooperation (ILAC) requirements or *self-declaration*[1] documentation about conformance to this standard regarding their OCR calibration and characterisation activities. **[DR5 in D2]**

The basic requirements of ISO 17025 [18] or CIPM MRA documents involve at least the following:

- qualified personnel, with regular competence monitoring.
- facilities with a controlled environment (e.g. temperature and humidity control, dark rooms with low stray light level).
- permanent presence and redundancy of measurement standards and instrumentation.
- firm traceability to SI by regular calibrations and checks between calibrations of all significant instruments used for cal/char activities.
- defined cal/char procedures, including relevant protocols for characterisation of OCR.
- uncertainty budgets compiled and evaluated according to the cal/char procedures of the laboratory.
- regular participation in relevant inter-comparison measurements.

This set of requirements must be present for each parameter for characterisation as listed in Table 4-1. Laboratories to be considered FRM compliant do not necessarily need to be formally accredited to ISO 17025. However, the principles of quality control as established by the standard must be fully followed for validated traceability and uncertainty budgets. Self-declaration shall include regularly updated documentation covering all points listed in Table 4-1, which are presented clearly and with sufficient details. It is noted that to comply with the FRM requirements, the formal accreditation of such a laboratory to ISO 17025 is not strictly required. However, the laboratory must follow the requirements of ISO 17025 and must be ready to provide proof of that at all times [17], [19], [20]. Regular participation in comparison experiments is an essential tool to achieve this.

Table 4-1. Minimum content of the self-declaration documentation for FRM labs [18].

Requirements for laboratories	**ISO 17025**	**Requirement in D-2**
Requirements for the competence of personnel (qualification, training, supervision, authorisation, monitoring the competence)	6.2	Appendix B
Requirements for environmental conditions in a lab (suitability for lab activities, documented requirements, control/monitoring of conditions, access to laboratory)	6.3	IR1 – IR9
Access to principal measurement equipment needed for cal/char activities (documentation, handling, sufficient accuracy, validation of performance)	6.4	DR2
Calibration program for the measurement equipment, which shall be regularly reviewed and adjusted; labelling of instruments according to their calibration status	6.4	DR2
Traceability charts for all relevant measurements to ensure that results are traceable to SI units	6.5	DR4
Description of procedures, including detailed measurement models (appropriate updated documentation, validation, proper performance)	7	DR3
Relevant uncertainty budgets for all principal measurements	7.6	DR3
Reports on comparison exercises, analysis of comparison results	7.2	OR2
Description of internal quality procedures to maintain the conformance with requirements of the self-declaration to ISO 17025	-	DR5

[1] "Self-declaration to ISO" is not just a statement from a cal/char lab. All requirements of the standard (or other additional relevant document) apply. The conformance must be presented on a relevant forum or must have passed an external audit. The difference from accreditation is that the process is not done by a dedicated authorized (ILAC) body.

5. General requirements for measurements

General requirements for calibration and characterisation of FRM OCR are listed in Table 5-1.

Table 5-1. General requirements for calibration and characterisation of FRM OCR.

Requirements for measurements	**Requirement in D-2**
Use of these harmonised laboratory guidelines calibration and characterisation of OCRs; Relation to community-wide management practices shall be shown, including results of comparison exercises	CR1 DR6 DR7
All data shall be in SI units with uncertainties estimated according to ISO GUM principles	CR2, DR3
Documented SI traceability of measurement results shall be present	CR2
A measurement model described clearly and with sufficient details	DR3
Calibration and characterisation certificates shall conform to ISO 17025 standard	DR4
Laboratories issuing certificates shall demonstrate their conformance to ISO 17025 standard	DR5
Regular participation of the OCR and the measurement scientist/team in relevant comparison exercises.	OR2

6. Description of calibration methods

6.1. List of calibration and characterisation activities

The complete calibration and characterisation scheme for the two most common OCR types (TriOS RAMSES and Sea-Bird Scientific HyperOCR) was planned by following the guidelines of the IOCGG protocols [2] and the measurements performed in FRM4SOC Phase-1 [10]. The list of calibrations and characterisations, its relation to the IOCCG Protocols and more significant differences are presented in Table 6-1. Even if calibration and characterisation of DALEC is still in exploratory phase, this Table should be equally valid for this instrument.

Table 6-1. List of calibrations and characterisations of hyperspectral OCR and relation with the IOCCG Protocols.

Parameter	Requirement in D-2	Section	Relation with the IOCCG Protocols	
			Level of agreement	Differences
1. Absolute calibration for radiometric responsivity	IR1	7	In agreement	No
2. Long term stability	IR1	N/A	Mostly in agreement	Minor, and subject to the available data (number and distribution of data points).
3. Stray light and out of band response	IR2	8.1	Mostly in agreement	More application methods
4. Immersion factor (radiance, irradiance)	IR1	8.2, 8.3	In agreement	No
5. Angular response of irradiance sensors in air	IR3	8.4	Mostly in agreement	Fixed azimuth angle, between routine char measurements regular checking against reference signal
6. Response angle (FOV) of radiance sensors in air	IR3	8.5	In agreement	No
7. Non-linearity	IR4	8.6	Mostly in agreement	Based on different integration times, test of thermal sensitivity, validation with monochromatic source
8. Accuracy of integration times	IR4	9	In agreement	No
9. Dark signal	IR7	8.7	Mostly in agreement	Using dark signal determined with the longest integration time
10. Thermal sensitivity	IR5	8.8	Mostly in agreement	Simultaneous recording of data for nonlinearity, dark signal, SNR, wavelength scale, etc.
11. Polarisation sensitivity	IR6	8.9	Mostly in agreement	Between routine char measurements checking against reference signal
12. Temporal response	IR8	8.10	TBD	
13. Wavelength scale	IR9	8.11	Mostly in agreement	Mostly in agreement
14. Signal-to-noise ratio	-	8.12	Mostly in agreement	Extended from the spectral to the instrumental properties
15. Pressure effects	IR1	7	TBD	

6.2. Irradiance calibration

Irradiance standard sources are 1000 W quartz tungsten halogen (QTH) lamps, also “FEL lamps” according to ANSI designation. FEL lamps are used at the standard calibration distance of 500 mm measured from their reference plane (or at the other standard distance if provided in the calibration certificate: PTB for example is calibrating lamps at the distance of 700 mm [21], [22]). If longer distances than stated in certificate are sometimes used by the labs due to the geometrical constraints, re-calculation of the irradiance to the used distance shall be metrologically supported and documented. All lamp models from different manufacturers are accepted for cal/char activities. However, it is extremely important to use each lamp according to its manufacturer's specifications. This

applies to the alignment process, ramp-up time and the operating current, supply voltage polarity and limited burn time - usually to less than 50 h - since its last calibration. In addition, the lamp information from the calibration certificate must be carefully studied to obtain information about ambient temperature during the calibration and the full width at half maximum (FWHM) of the instrument used for that calibration. Any QTH lamp can be used if the above-listed parameters are adhered to control. The QTH lamps with smaller filament sizes can be used at distances shorter than the calibration distance of 500 mm, but the finite dimensions of the filament and the radiometer's input aperture and related geometric deviation from the point source approximation must be considered. It is strongly recommended to perform the calibration at an ambient laboratory temperature between +20 °C and +25 °C. Calibration at lower temperatures shall be avoided due to possible thermal instability [23] of the cosine collector; calibration at higher temperatures shall be avoided due to rapid increase of the dark signal and due to respective decrease of the signal to noise ratio. The radiometer (or ambient) temperature must be monitored and logged. Heating of the radiometer and measurement setup by the lamp's radiation shall be avoided.

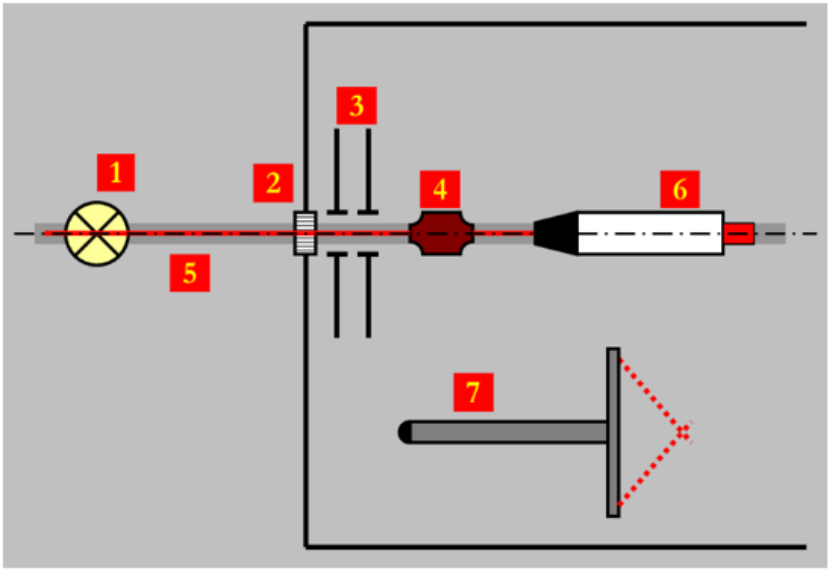

Figure 6-1. Irradiance calibration setup. 1 - FEL lamp; 2 – shutter; 3 – baffles; 4 - alignment laser; 5 - optical rail; 6 – radiometer; 7 – contactless distance probe.

Figure *6-1* presents a schematic of the irradiance calibration setup at UT. Other laboratories may have slightly different distance measurement, baffling, and power supply solutions. The baffling coatings shall be chosen to absorb the radiation in the full sensitivity range of the radiometers. Knife-edged apertures are preferred to minimize parasitic reflections. Each laboratory shall evaluate the measurement setup for ambient stray light, back-reflections, and thermal effects due to heating of the equipment by the radiation. However, the principle for the irradiance calibration is very well standardised.

The supporting equipment (electrical, distance, temperature measurement devices and so on), relevant to the evaluation of the measurement results and uncertainties, shall be calibrated and traceable according to ISO 17025. For the lamps calibrated with their enclosure, the latter must also be used during the cal/char activities. During the measurements, the lamp current and voltage must be monitored and logged to get full information about the accuracy of the power supply, including a calibration certificate for the required shunt resistor. The measurements must be done at the certified lamp calibration distance, which is usually 500 mm. The distance is measured from the lamp reference plane defined in the calibration certificate. If the irradiance sensor saturates when it is illuminated by the lamp at the standard distance of 500 mm, and the reduction of gain or integration time is not possible/justified, it is necessary to reduce the irradiance level by increasing the distance as described in the section 3 of the IOCCG Protocols [2].

Multiple readings must be recorded, and dark measurements must follow the lamp measurements by blocking the direct light path from the lamp to the radiometer's input with a shutter. The shutter construction depends on the

measurement setup and amount of ambient stray light. For the instruments with an internal shutter (e.g. HyperOCR), the external shutter is only used to evaluate the ambient stray light effect. TriOS RAMSES, Seabird's and DALEC radiometers must be switched on at least 20 min before calibration measurements and record spectra with the integration time used during calibration to achieve a steady thermal state of the internal electronics of radiometers.

The main uncertainty sources that shall be accounted for in irradiance calibration are:

- lamp spectral irradiance (from the lamp's certificate).
- lamp current (monitored during the calibration).
- lamp ageing (model & experience).
- interpolation to the radiometer's wavelength scale (model).
- distance measurement (depends on the method and experience).
- reproducibility of the alignment (experience or direct experiment).
- ambient stray light (experiments with the measurement setup).
- the standard deviation of the light and dark signal.
- radiometer's temperature (thermal characterisation results, experience or manufacturer's statement).

When possible, the calibration measurements must be completed with two or more integration times to quantify the radiometric linearity of the irradiance sensor. The parameters that must be reported are listed in Annex A.

6.3. Radiance calibration

The typical radiance calibration procedures are based on the so-called lamp-plaque technique, where an FEL lamp with known irradiance is used to illuminate a reflectance standard with known reflectance and BRDF to account for the non-Lambertian behavior of the plaque or use an integrating sphere with known radiance. It is strongly recommended to perform the calibration at +20 °C to +25 °C. The radiometer (or ambient) temperature must be monitored and logged.

6.3.1. Calibration of radiance with a reflectance plaque

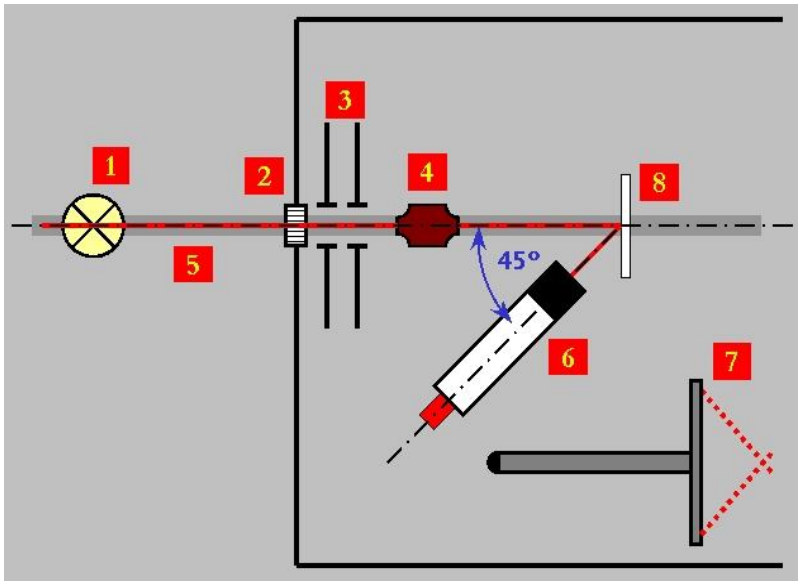

Figure 6-2. Spectral radiance calibration setup with lamp and plaque. 1 – FEL lamp; 2 – shutter; 3 – baffles; 4 - alignment laser; 5 - optical rail; 6 – radiometer; 7 – contactless distance probe; 8 – reflectance plaque.

A typical lamp-plaque radiance calibration setup is presented in *Figure 6-2*. Although the lamp-plaque radiance calibration setup is standardised (the reflectance plaque is illuminated at normal incidence using the irradiance

lamp and the transfer radiometers are set at 45° to the normal) there are still several factors that can vary between laboratories and some of them cannot be easily changed. The varying factors in this radiance setup include:

1. The distance between the lamp and the reflectance plaque. The lamp is calibrated at 500 mm. However, this distance is unfavourable in some cases for radiance calibration due to the high non-uniformity of the illumination patch (also known as vignetting) within the FOV of the radiometer. Also, physical dimensions of the radiometer might not support such a short distance. Thus, that distance is often increased, improving the uniformity of the illumination patch substantially. The drawback is that the distance-offset correction should be applied to the calculation of the lamp irradiance to account for the difference in the real filament position and the lamp reference plane that is used to measure the 500 mm lamp calibration distance. In these guidelines, the recommended distance shall be 1000 mm or larger, given that the uncertainty of the distance-offset correction contributes to the uncertainty budget less than the non-uniformity of the illumination patch at the standard distance of 500 mm.

2. The size of the reflectance plaque and the size of the illumination patch are defined by the apertures in the baffles. Impact on the calibration coefficients and on the associated uncertainties due to these size differences among the labs is expected to be negligible.

3. The distance between the reflectance plaque and the radiometer. This will define the size of the plaque that the instruments "see" during the calibration and the magnitude of back-reflection from the radiometer's input window to the plaque and back to the radiometer's input. In the case of the plaque-lamp setup, with increasing distance, the signal will decay for two reasons: smaller back-reflection and vignetting – non-uniform light field on the plaque. The corresponding uncertainty component could reach 0.5%. The radiometer adapter should allow movements of the radiometer along its optical axis to investigate the signal change with respect to the radiometer-to-panel distance. It is straightforward to install RAMSES and HyperOCR on the V-shaped holders while DALEC needs purpose designed adapter.

The reflectance standard should be calibrated for diffuse reflectance factor at 0°/45° geometry. However, the most common calibration is reflectance at 8°/h, which can be easily corrected for 0°/45° geometry for Spectralon™ reflectance targets. There is no strict rule for the recalibration time for the reflectance standards. However, using the standards that are clean upon visual inspection and have been used only in the laboratory environment is strongly recommended. It is well known that Spectralon™ can change its reflectance due to exposure to UV light and get dirty while used in field environments. As PTFE – main constituent of Spectralon™ plaques - has a phase transition at 19 °C, the Spectralon™ reference standards should not be used in lab conditions below 20 °C [23].

6.3.2. Calibration of radiance with an integrating sphere

The measurement setup with an integrating sphere is shown in *Figure 6-3*. In the case of an integrating sphere, the size of the sphere and the size of the port, uniformity of that port and the sphere flux level might vary. An integrating sphere can be calibrated directly for radiance, and then the calibration certificate will state the area of the entrance port that was measured during the calibration. If the radiometer under the test has a significantly larger FOV, correction must be applied to account for that difference. The operating conditions of the lamp (including the electrical parameters and the burn time since the last calibration) apply in the same way as in the case of irradiance calibration.

Some integrating spheres may not have a radiance calibration but a transfer radiometer that is used to calibrate its radiance. It is recommended to follow the calibration procedure described in [2], [24]. The stability of that radiometer, FOV, and spectral characteristics must be known to account for the difference between the transfer radiometer deriving the radiance calibration and the radiometers that will be used in this comparison. The transfer radiometer must have a valid, SI traceable calibration (as compliant to the effective quality management system in the laboratory).

The radiometer's fore optics will reflect a part of the signal back into the sphere. The effect can be checked when changing the distance between the radiometer and the sphere. The signal will smoothly decrease when increasing the distance until the diameter of the sphere's output port gets equal to the FOV of the radiometer, and the signal starts dropping significantly. Corresponding uncertainty due to back-reflection can reach up to 0.5%.

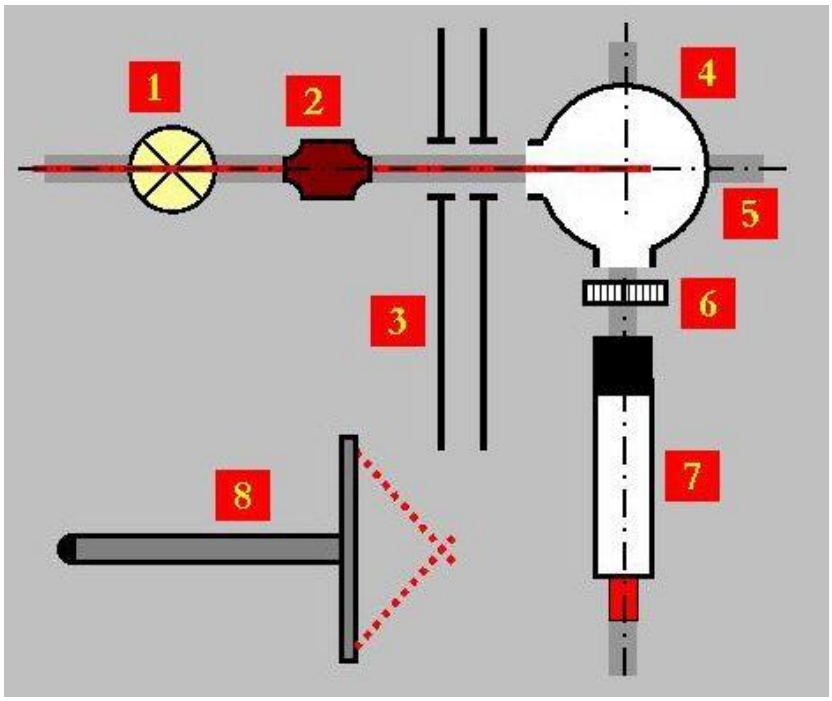

Figure 6-3. Spectral radiance calibration setup with integrating sphere. 1 - lamp, 2 - alignment laser, 3 - baffles, 4 - integrating sphere, 5 - optical rails, 6 - shutter, 7 - radiometer, 8 - distance probe.

6.3.3. Uncertainties

The main uncertainty sources that shall be accounted for in radiance calibration are:

- the uncertainty components as listed for irradiance calibration.
- the plaque reflectance (from plaque's certificate).
- plaque ageing (calibration history & experience).
- plaque alignment reproducibility (experience & experiment).
- plaque illumination non-uniformity (experiment & literature).
- back reflection (experiment).

The reported parameters are listed in Annex A.

7. Description of characterisation methods

7.1. Spectral response/stray light matrix

The centre wavelength (CWL) and bandpass of each band shall be characterised for any radiometer [2]. The wavelength scale can be validated/established by line sources such as low-pressure discharge lamps and lasers. In the case of typical OC radiometers with a bandwidth of about 10 nm, CWL, bandwidth, and stray light can also be characterised by using a scanning monochromator with a wavelength setting error of <0.2 nm. The spectral response function determines these parameters, i.e., the passband, for each channel with a scanning monochromatic source exhibiting no stray light (based on specifications provided by the monochromator manufacturer) and with a bandwidth significantly less than the expected bandwidth of the tested radiometer. In the proposed measurement sequence, the monochromator is iteratively tuned around the expected CWL until reaching the symmetric signal output (i.e. signal of the neighbouring pixels on both sides of the maximum do not differ by more than 20% from each other). For lower spectral stray light, using of double scanning monochromator

is needed. Both the QTH lamps and short arc Xe lamps can give satisfactory results as the light source. Using the tunable lasers, when available, is preferred from the SNR point of view. However, characterization of nearly all pixels is still necessary as interpolation of the line spread functions leads to significant distortions in most cases. In the case of array-like OC radiometers such as the three considered classes, the temporal stability of the light source is less significant as the full spectrum is recorded at once. Due to the rather low intensity of the monochromatic output, multiple spectra must be averaged. The dark signal must be handled according to the radiometer class. Response functions are normalised to the maximum value to be equal to 1.0. The (nominal) centre wavelength is then determined as the wavelength halfway between those at which the normalised response is 0.5. The bandwidth is defined as the passband determined by the full width at half-maximum (FWHM) intensity points.

In the case of significant distortions, the shape of the radiometer's bandpass, the central part must be scanned with bandwidth and spectral step at least 10 to 20 times smaller than the characterised bandwidth.

In *Figure 7-1*, the measurement setup for characterisations of stray light patterns is shown. The entrance slit of the monochromator must be filled precisely to avoid the stray light (overfilling) and signal loss (over- and underfilling). Lens 2 is chosen to maximize the power through the monochromator and to fulfill the monochromator's aperture. The output optics can be avoided in most cases, providing the entrance of the radiometer is placed exactly behind the exit slit of the monochromator. The output radiation from the monochromator should be converted by using lenses/mirrors to closely match the field conditions, i.e. overfilling the entrance aperture. However, especially in the case of irradiance sensors, overfilling of the aperture might reduce the signal levels below acceptable. Ambient stray light must be suppressed by baffles and covers. It is advisable to use a fully automatic monochromator under computer control as the full measurement sequence may take up to 10 hours.

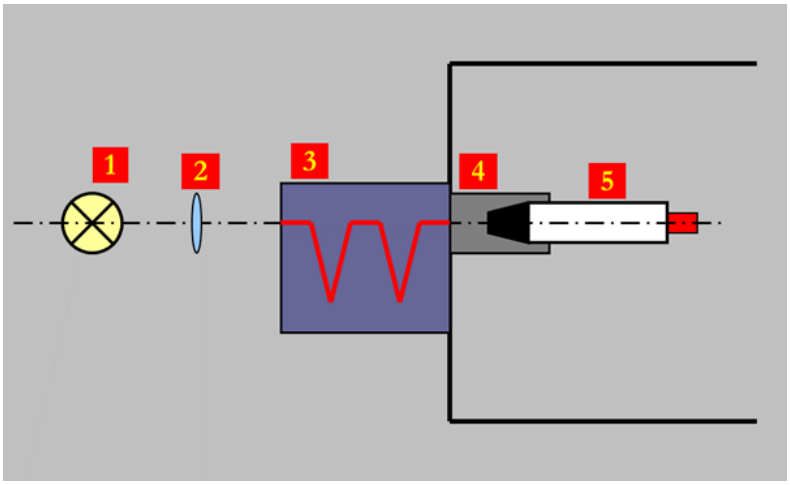

Figure 7-1. Schematic diagram of the measurement setup for characterisation of stray light pattern. 1 - ribbon filament lamp; 2 - lens; 3 - double monochromator; 4 - adapter; 5 – radiometer.

The averaged, linearity-and-dark-corrected spectra called line spread functions (LSF) are organised into the Stray Light Matrix (SLM) so that the horizontal axis contains excitation wavelength (the monochromator set point) and the vertical axis - the LSF wavelength (*Figure 7-2*). In the case of typical OC radiometers, the LSF should be measured for as many pixels as possible, considering the sensitivity decay at both ends of the spectrum. An example of the SLM is shown in *Figure 7-2*.

The reported parameters are listed in Annex A.

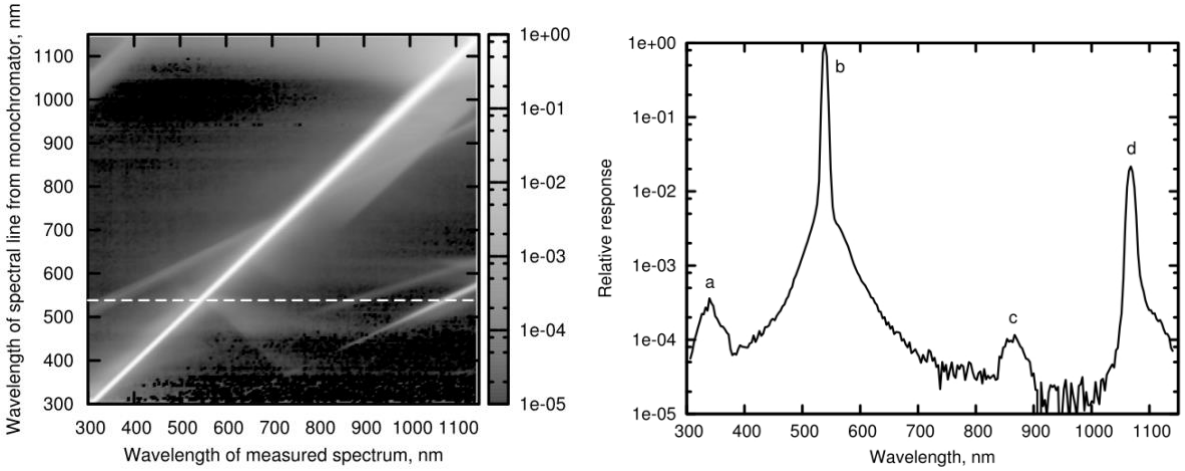

Figure 7-2. Stray light matrix and an example LSF of an OC array radiometer. The dashed line on the left pane corresponds to the LSF on the right pane.

The inversion of the "modified" SLMs provides the basic method for stray light corrections [25], [26]. Before the inversion method, the "modified" SLM must be obtained. At first, the diagonal and surrounding elements of the original SLM within the instrument's bandpass are set to 0, thus isolating the influence of the stray light correction from the bandpass region. After that, the SDF is calculated normalizing the LSF outside the bandpass by the total signal within the bandpass of a spectrograph. Finally, to get the "modified" SLM suitable for the matrix inversion method the respective identity matrix of the same size with the SLM is added. However, in some cases, the iteration method by using SLM is still more effective [27], [28] as it uses also the SLM information of the bandpass region. The stray light characterisation is a demanding task. Some commercial instrument suppliers deliver spectrometers with stray light correction matrices built into their processing software. As suggested by [29], class-based characterisations can be considered for commercial instruments used in validation activities. However, although the tested instruments so far (based on Zeiss MMS-1 module) had similar stray light features, a class-specific approach may fail for some applications (i.e. may not constraint the uncertainty levels below the threshold that the given application demands) due to individual differences in pixel-to-wavelength scales.

7.2. Determination of immersion factors for irradiance sensors

Both sections 7.2 and 7.3 follow very closely what is described in Section 4 of the IOCCG protocol chapter 3 [2], with a few minor editorial changes but no actual difference in content. Very few results are published, and independent repeating of characterisations according to the IOCCG recommendations is needed for validation.

Immersion factors account for responsivity variations resulting from changes in the refractive index of the medium in contact with the fore optics (*i.e.*, the cosine collector and the optical window for irradiance and radiance sensors, respectively) [2]. Determination of the immersion factors apply to the radiometers that can potentially be used underwater in the field (RAMSES, HyperOCR, not the case for DALEC).

When a diffuser is immersed in water, the measured transmissivity of the water-diffuser system is less than that of the air-diffuser system. Consequently, if an instrument is calibrated in air, a correction (i.e., the immersion factor) for the change in transmissivity must be applied to irradiance responsivity coefficients for underwater measurements [2].

The change in transmissivity of a collector when immersed is the net effect of two separate processes, both depending on the relative difference in refractive indices between the diffuser material (e.g., fused silica) and the surrounding medium (i.e., air or water). The first is due to a change in the reflection of light at the external medium-collector interface; the second is due to a change in the reflection of light at the inner (*i.e.,* inside the diffuser) collector-medium interface [2].

The refractive index of a collector material is always greater than that of both water and air. In addition, the refractive index of water is greater than that of air, so the Fresnel transmission of the water-diffuser interface is greater than that of the air-diffuser interface. Therefore, the initial transmission of light into the irradiance collector is greater in water than in air. However, the transmission of light out of the diffuser into the surrounding medium is greater in water than in air. Therefore, a larger fraction of the light scattered within the diffuser passes back into the water column than what would pass back into the air. Because the gain in the leaving flux exceeds the gain in the incoming flux, the net effect of these processes is a decrease in the transmissivity of the immersed collector [30].

Previous investigations have shown that the immersion factors for irradiance sensors must be characterised experimentally. In fact, some manufacturers only characterise prototypes with a particular collector design and material specification, then successively provide nominal immersion factors for all production radiometers using that collector design. In this respect, [31] applied the characterisation procedure with repeatability of better than 1% and observed root-mean-square differences between immersion factors of radiometers from the same series exceeding several per cent, with values as large as 10% in some spectral bands, which suggests the inapplicability of the nominal immersion factors.

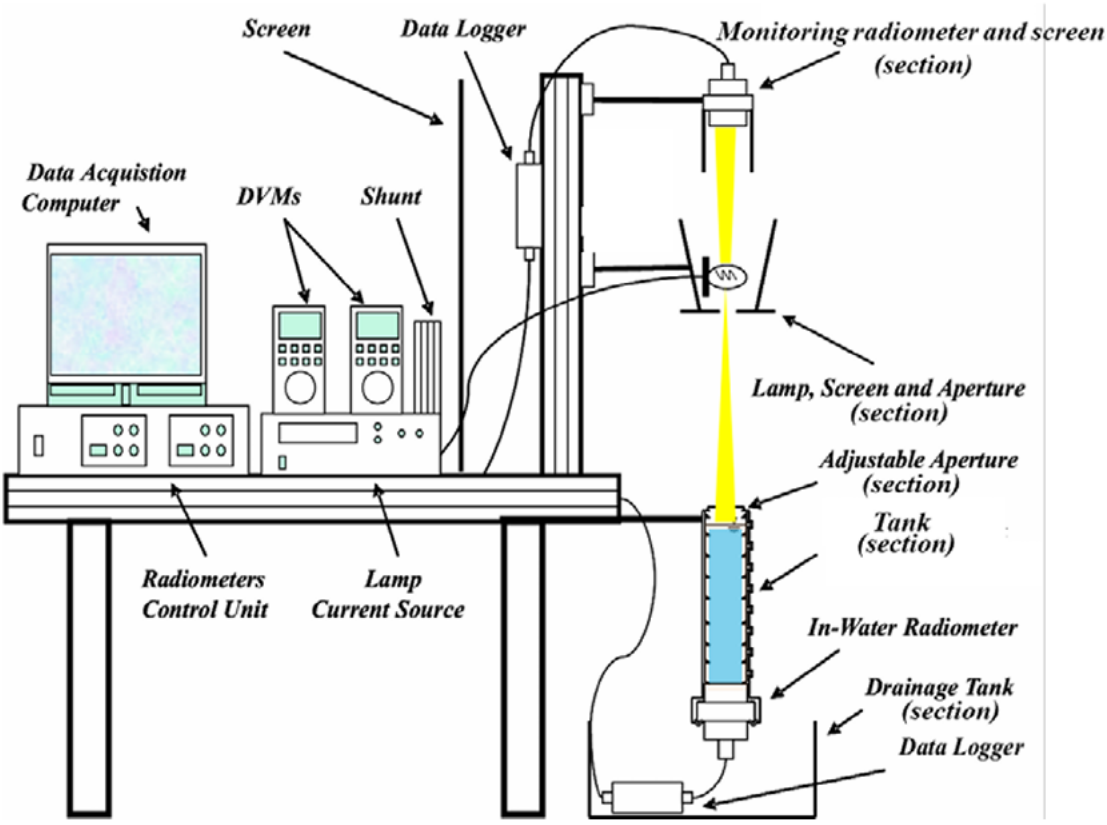

Figure 7-3. Schematic diagram of the measurement setup for determining the immersion factor for irradiance sensors. Figure taken from [2].

The diagram of the measurement setup for irradiance sensors is given in *Figure 7-3*. The small tank size, which allows for the use of affordable quantities of pure water, requires an efficient internal baffling to minimize stray light. A suggested procedure to measure the immersion factor [2] shall be realised as follows:

1. The instrument is placed in a water tank with the irradiance collector levelled and facing upward.
2. A tungsten-halogen lamp with a small filament (to mimic a point source), powered by a stable power supply, is applied as a light source. The measurement system (lamp, radiometer, and water vessel)

must be carefully aligned, and the lamp's distance above the irradiance collector's surface must be carefully measured. After lamp warm-up, an initial reading is taken in the air before raising the water level in the tank above the dry collector. Lamp voltage and current should be monitored throughout the characterisation to ensure a stable output. In addition, the output flux must be continuously monitored with a separate in-air irradiance sensor to ensure lamp stability. The water temperature must also be recorded to determine the water refractive index accurately.

3. The water is raised initially to a carefully measured level z above the collector surface, and the radiometer outputs are recorded for all bands. To achieve the repeatability of better than 1% implies careful attention to the cleanliness of the water and removal of any air bubbles from fore optics. It is thus recommended to use pure water and a relatively small water tank with an efficient internal baffling.
4. The water level is then increased stepwise, e.g., in 5 cm increments, and the instrument response is measured and recorded for each depth z. A maximum water depth of a few dm (e.g., 40 cm) is normally adequate to obtain data covering a sufficient response range.
5. The water level is then lowered, and data is recorded over a similar series of incremental depths.
6. A final reading is taken with the water level below the collector after drying it.

A minimum water depth of tentatively 5 cm is recommended to avoid artefacts caused by multiple reflections between the collector and air-water interface. These reflections would increase the transmitted flux and therefore decrease the apparent immersion effects. The magnitude of this artefact increases with a decrease in the minimum depth and an increase in the diameter of the collector.

The amount of flux arriving at the collector varies with the water depth and is a function of several factors:

- The attenuation at the air-water interface, which varies with wavelength.
- The attenuation over the water path-length, which is a function of depth and wavelength.
- The change in the solid angle of the light leaving the source and arriving at the collector, caused by the light rays changing direction at the air-water interface, which also varies with wavelength and water depth.

Using the Fresnel reflectance equations and taking the index of refraction of air as one, the normal transmittance through the water surface is

$$T_S(\lambda) = \frac{4 \cdot n_w(\lambda)}{[1 + n_w(\lambda)]^2} \tag{1}$$

where $n_w(\lambda)$ is the index of refraction of the water at wavelength λ.

The change with water depth z of the refracted solid angle subtended by the collector, as viewed from the lamp filament, is given by

$$G(z, \lambda) = \left\{1 - \frac{z}{d}\left[1 - \frac{1}{n_w(\lambda)}\right]\right\}^2 \tag{2}$$

where d is the distance of the lamp source from the collector surface.

The immersion correction factor for irradiance is then calculated as [2]

$$F_{i,E}(\lambda) = \frac{DN_a(0^+, \lambda)}{DN_w(0^-, \lambda)} T_S(\lambda) \tag{3}$$

where DN_a and DN_w are in-air and sub-surface irradiances in digital counts corrected for the dark signal. The latter value is determined from the least squares fit as a function of the water depth z_i above the collector of $ln[DN_w(z_i, \lambda)/G(z, \lambda)]$.

The factor $G(z, \lambda)$ corrects for the geometric effects induced by the change in the solid angle of the light leaving the source and arriving at the collector after crossing the air-water interface.

For lab measurements, purified water shall be used [2]. The actual application of lab-measured $F_{i,E}(\lambda)$ values to field measurements then requires corrections accounting for differences in the refractive indices between pure and natural waters as a function of salinity and temperature. Because of the difficulty of generating and working with pure seawater, the correction to account for salinity and temperature effects can only rely on experimental

estimates of the correction factor to be applied to the pure water calibration. This approach, however, is not expected to appreciably increase the uncertainty assigned to the experimental determination of $F_{i,E}(\lambda)$.

The reported parameters are listed in Annex A.

7.3. Determination of immersion factors for radiance sensors

Similarly to irradiance sensors, the absolute calibration for spectral radiance sensors is performed in air. Thus, when the instrument is submerged in water, a change in responsivity occurs, and a correction must be applied. This change in responsivity is caused by i) a change in transmission through the water-window interface with respect to the transmission of the air-window interface, and ii) the change in the solid angle FOV relative to that in air.
Since $n_w(\lambda)$ is a function of wavelength, the correction factor $F(\lambda)$ is also a function of wavelength. Given that the refractive index of air can be taken as unity at all wavelengths, it is $n_g(\lambda)$ the index of refraction for the material constituting the optical window of the radiance sensor, the correction for the change in transmission through the window, $T_g(\lambda)$, is given by

$$T_g(\lambda) = \frac{\left[n_w(\lambda) + n_g(\lambda)\right]^2}{n_w(\lambda)\left[1 + n_g(\lambda)\right]^2} \tag{4}$$

and the correction for the change in FOV is

$$F_v(\lambda) = [n_w(\lambda)]^2. \tag{5}$$

For an optical window made of fused silica, the spectral refractive index can be computed using an empirical fit to the Hartmann formula, as

$$n_g(\lambda) = 1.4424 + \frac{7.1661}{\lambda - 144.717} \tag{6}$$

where λ is in nm. Manufacturers provide refractive indices for different materials commonly used for optical windows (e.g., BK-7 - a high-quality optical glass).

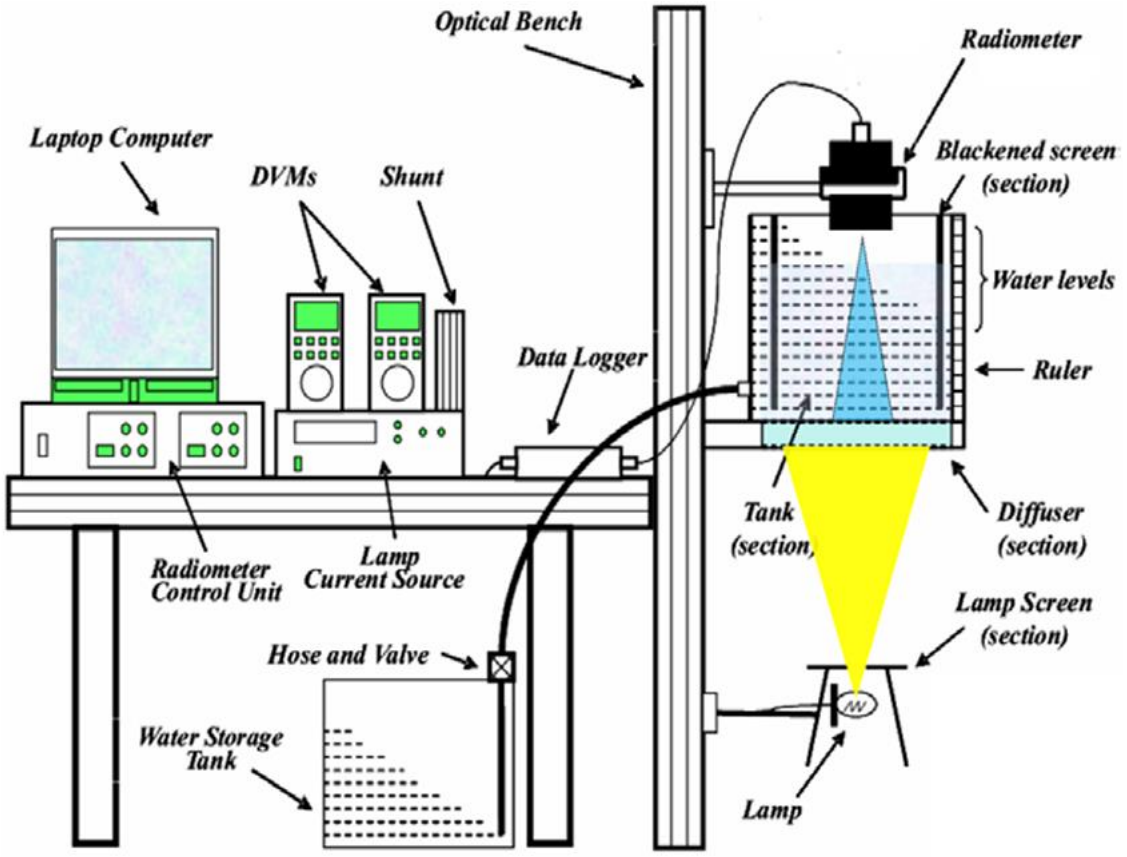

Figure 7-4. Schematic diagram of measurement setup for determining the immersion factor for radiance sensors. Figure taken from [2]*, see* [32].

An experimental characterisation of a class of OCRs has shown a negligible variation of the immersion factor among sensor units [32]. However, theoretical and experimental determinations exhibited appreciable differences for some radiometer series [33]. Following the method proposed by [32], the experimental characterisation of immersion factor for radiance sensors is made using in-air and in-water radiance measurements successively, performed at a constant sensor–source distance with the sensor looking vertically down at a stable, homogeneous, and near-Lambertian source (diffuser) immersed in pure water. The measurement procedure is equivalent to that for the immersion factor for irradiance sensors, except that immersed measurements are taken with a single distance r between the optical window and source while multiple in-air measurements are taken for decreasing the water level z_i and, thus, with diverse water depths $r - z_i$ between the water surface and the optical window (see the schematic of the measurement setup in *Figure 7-4*).

Following [32] $F_{i,L}(\lambda)$ is determined from

$$F_{i,L}(\lambda) = \frac{DN_a(0^+,\lambda)}{DN_w(0^-,\lambda)} \frac{\Omega_a}{\Omega_w(\lambda)} \frac{1}{T_S(\lambda)} \tag{7}$$

where DN_a and DN_w are the digital values related to the above- and in-water radiances corrected for the dark-signal. DN_a is computed as the intercept of the least-squares fit to the distance z_i of the optical window from the water surface, regressed with the log-transformed in-air measurement $DN_a(r - z_i, \lambda)$.
The terms Ω_a and $\Omega_w(\lambda)$ are the in-air and in-water solid angle FOVs, respectively: their exact values are not needed because their ratio is known:

$$\frac{\Omega_a}{\Omega_w(\lambda)} = n_w^2(\lambda) \tag{8}$$

$T_S(\lambda)$ is the normal transmittance through the water surface given by (1). However, if the sensor FOV is larger than a few degrees, $T_S(\lambda)$ should be replaced by the mean of the water surface transmittances determined over the solid angle $\Omega_w(\lambda)$.

The diffuse light source can be obtained with an LCD flat-field source operated underneath a water tank with the bottom made of a transparent material (e.g., optical glass), or alternatively, a number of quality diffusers illuminated by a halogen-tungsten lamp operated at an opportune distance to increase the homogeneity of the resulting diffuse source [34]. This latter solution provides a more uniform spectral distribution of light in the visible and near-infrared spectral region [35].

The reported parameters are listed in Annex A.

7.4. Determination of angular response of irradiance sensors in air

For determination of the angular response, a pseudo-collimated light beam is needed. Such beam could be formed by using a point source with collimating optics using lenses, spherical or parabolic mirrors or the bare point source far enough from the radiometer's input diffuser. The latter is practically useless due to too low irradiance levels for most of the OC radiometers. The collimated beam defines the optical axis of the setup. The positioning of the radiometer in the angular characterisation setup is shown in *Figure 7-6 and Figure 7-7*. The initial azimuth (φ=0) corresponds to the horizontal alignment of the face of the hexagonal nut of the connector closest to the red dot while the red dot points upwards (see *Figure 7-6*). The radiometer should be rotated in the horizontal plane coplanar to the optical axis so that the crossing of the optical and rotation axes stays in the centre of the diffuser's surface (*Figure 7-7*). The figures and explanations below correspond to the vertical rotational axis. For an ideal diffuser, the radiometer's output signal should follow the cosine law with respect to the rotation angle θ over all wavelengths and azimuthal angles φ of the radiometer. Ideally, the optical axis shall be defined by the center of the diffuser, not the cylindrical body of the radiometer, in the case of misplacement of the diffuser. However, in the case of the radiometers in this document, the misplacement of the diffuser is insignificant.

The angular response of RAMSES irradiance sensors is often asymmetrical (D-7) [36]. To guarantee reproducibility of characterisation results, for angular measurements of RAMSES irradiance sensors, the sensor's azimuth angle shall be clearly defined and specified in the characterisation report. The zero azimuth shall be pre-defined by the radiometer's user or measuring laboratory and must be clearly stated in the measurement reports. This can be adjusted by -using a small bubble level placed on the connector (see *Figure 7-6*, corresponding to a radiometer with cylindrical symmetry, such as is the case for TriOS RAMSES and Seabird's HyperOCR). The order in which the scanning angles θ and φ are varied can be arbitrary, but the final data should be presented in accordance with *Figure 7-6* and *Figure 7-7*.

Figure 7-5. Images of the single-coiled filament of an incandescent halogen lamp formed by a double-convex lens (focal length f= 200 mm) depending on the distance between the lamp and the lens. Left: f +0 mm, middle: f -25 mm, right: f +40 mm.

The practical considerations are as follows. First, the ideal point source does not exist, and the images from the practical sources (filaments, gas discharges) will show spatial and wavelength-dependent structure when collimated (*Figure 7-5*). Evaluation of the spatial uniformity of the beam is strongly advisable. The small (e.g. 3 × 8 mm in the case of a 250 W QTH lamp) filament can be considered a reasonably good point source even without collimation when the distance from the lamp to the radiometer exceeds ~1 m. However, the irradiance levels at the diffuser drop significantly compared to the collimated beam, resulting in the need for long integration times. Second, proper baffling of the beam is needed because the bright sources create strong reflections on the nearby surfaces (lamp sockets, housings etc.). Reflections from the edges of the baffles can severely distort the beam geometry. UT uses diaphragms made of thin anodised aluminium foil or knife-edge apertures placed as close to the lamp as possible, in case needed. In the case of insufficient baffling, the radiometer can collect a significant amount of light scattered from the lab's structures, especially at incident angles close to 90°. Evaluation of the spatial uniformity of the beam is strongly advisable to assess the effectiveness of the baffling. Third, the results are extremely sensitive to small misalignments. The effect can be checked by repeating the full alignment and validating against the opposite azimuth (i.e. rotating the radiometer around its axis by 180°).

A dual-beam laser can be used to align the lamp and mount the radiometer on the rotating stage. The radiometer's adapter should include enough degrees of freedom to perform the alignment (*Figure 7-8*). The alignment process, in general, consists of the following steps and should be iteratively repeated until a satisfactory result:

- align the rotation axis so that it would not deviate from the optical axis when changing θ in the range $-90° < \theta < +90°$.
- align the centre of the diffuser on the optical axis, near the rotational axis.
- by using back-reflection, set the radiometer's longitudinal symmetry axis parallel to the optical axis.
- rotate the table to ±60° and shift the radiometer along its axis to centre the laser beam spot.
- align the lamp to the optical axis.
- align the collimating optics, if used.

The results are expressed as deviation from the cosine law (as defined in detail in [2]) for the two perpendicular azimuthal planes (0°/180° and 90°/270°, respectively), and for at least 10 rotational angles (θ=0°, ±15°, ±30°, ±45°, ±60°, ±75°), normalised to θ=0° and four wavelengths (nearest pixels to): 400 nm, 550 nm, 700 nm and 850 nm. It is advisable to measure the θ=0° before/after every θ set point to reduce the differential thermal effects between the different angular configurations in the radiometer. The lamp stability must be monitored or ensured to stay within ±0.1% between taking the readings at angle θ and the corresponding θ=0° reading. To avoid possible integration time and linearity issues, the integration time of the radiometer shall be fixed (determined by the θ=0° reading).

The reported parameters are listed in Annex A.

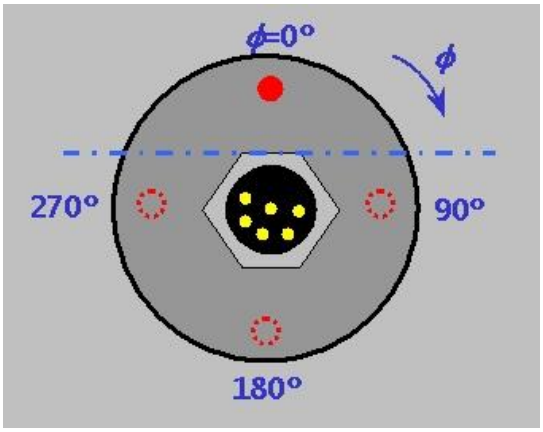

Figure 7-6. Positioning of the radiometer (as seen from the connector's side). The dashed blue line indicates where the small bubble level should be positioned to determine the azimuthal alignment in case of cylindrical symmetry.

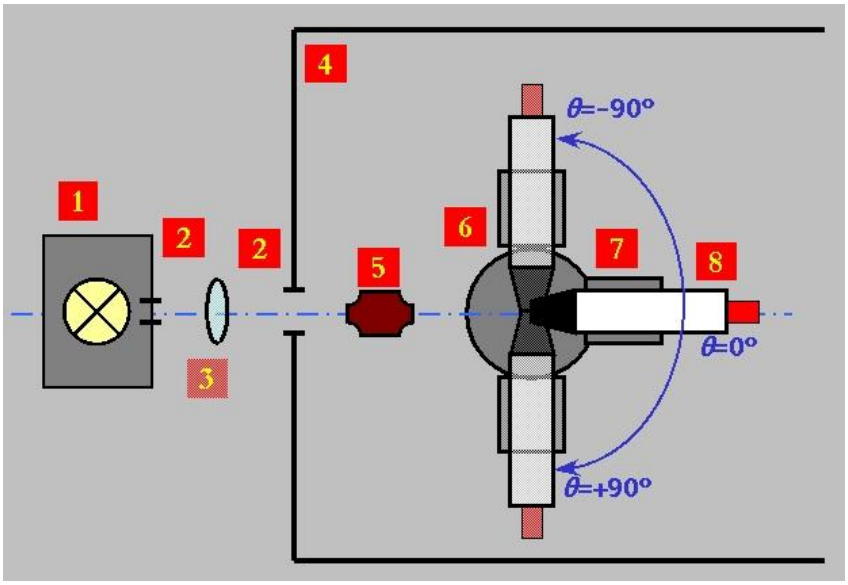

Figure 7-7. Measurement setup for the characterisation of the angular response of irradiance sensors (view from above). 1 - lamp; 2 - diaphragms; 3 - lens; 4 - detector compartment; 5 – alignment laser; 6 - rotating stage; 7 - adapter; 8 - radiometer.

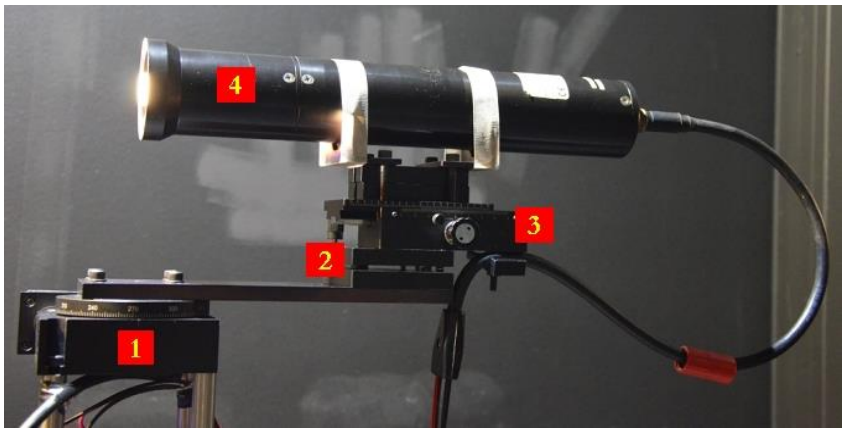

Figure 7-8. Angular measurements. 1 - rotating stage; 2 – tilt + rotation; 3 - longitudinal shift; 4 - radiometer.

7.5. Measuring FOV of the radiance sensors in air

The angular characterisation setup described in chapter 8.4 can be used for FOV measurement, but without the lens 3 (*Figure 7-7*)), and setting the distance between the lamp and the radiometer is sufficient to avoid overexposure. The geometric conventions for alignment are similar to those shown in *Figure 7-6* and *Figure 7-7*) for instruments with cylindrical symmetry such as SeaBird/HyperOCR and TriOS/RAMSES. For IMO/DALEC, a specialized adapter is needed for the alignment. It is proposed to determine the field of view for two perpendicular azimuthal planes, 0°/180° and 90°/270°, respectively. The result is not sensitive to the scanning direction θ and the small offsets of θ. Typically, a 250 W QTH lamp with two apertures is sufficient at the distance between the lamp and the radiometer, approximately 3 m. The alignment of the setup is like the alignment of the irradiance sensor.

The FOV is calculated as the full width at half the maximum of the measured response with respect to the rotational angle θ. The full maximum is taken at θ=0° and not at the actual maximum, which might happen within the FOV. The results should be presented for both azimuthal planes and all recorded azimuths.

The reported parameters are listed in Annex A.

7.6. Determination of the non-linearity

To determine the radiometric non-linearity, a stable source (e.g. the calibration source) must be measured using two different integration times. This can be done during the radiometric calibration. Data averaging and dark measurements must be applied accordingly. The corrected spectrum $S_{1,2}(n)$ is calculated as

$$S_{1,2}(n) = \left[1 - \left(\frac{S_2(n)}{S_1(n)} - 1\right)\left(\frac{1}{t_2/t_1 - 1}\right)\right] S_1(n), \tag{9}$$

where $S_1(n)$ and $S_2(n)$ are the raw signals of pixels $n \in (0{,}255)$, measured with integration times of t_1 and t_2, respectively, after scaling up to the largest used integration time. The corrected signal $S_{1,2}(n)$ is shown to be independent of the selection of t_1, t_2 and virtually corresponds to the reference integration time of 0 ms. This is valid if the error of the integration time is negligible (as it is the case with the two major instrument classes in this document) and demonstrated in [37]. The standard deviation of $S_{1,2}(n)$ is substantially determined by the signal with the shortest integration time. Unfortunately, using a single lamp source limits the useful spectral range for the non-linearity correction determined. An alternative (more precise but more demanding) method can be achieved by using a stable, adjustable monochromatic source set to the central wavelength of the certain (measured) pixel of the radiometer. Re-adjusting at each measured wavelength suitably the radiation intensity and the integration time of the radiometer, a more effective selection of signal level and, as a result, better signal-to-noise ratio in UV and NIR parts of the spectrum can be achieved. However, such non-linearity characterisation is much more time-consuming as the full spectral range must be measured pixel by pixel. *Figure 7-9* shows the difference between non-linearity coefficients α determined by using both methods. During radiometric calibration, the coefficient α has been determined in 2018 and twice in 2022. Determination of the non-linearity coefficient α by using an adjustable monochromatic source is made in 2022. In the central part of the spectrum (between 450 nm and 700 nm), the agreement between determinations is satisfactory. In the UV and NIR parts, determination by using an adjustable monochromatic source is clearly preferable and can be considered as validation/reference of the full-spectrum results.

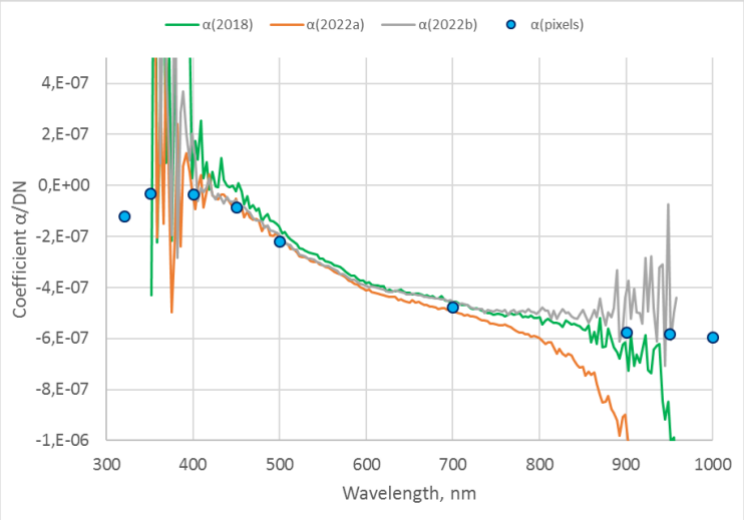

Figure 7-9. Non-linearity coefficient α of a RAMSES sensor (SAM 821E) determined during calibration (continuous lines) and by using an adjustable monochromatic source (blue points).

For the setup, pre-heating and uncertainty, consider the guidelines in sections 6.1 and 6.3. As the radiometric non-linearity lies typically between 0% and 2%, special care must be taken to avoid temporal drifts mainly caused by lamp instability and changing temperature of the radiometer. For example, acquiring with integration times t_1 and t_2, the measurement sequence must be t_1-t_2-t_1-t_2-t_1 (each measurement containing at least 10 readings), followed by corresponding dark measurements with t_1 and t_2. The sequence can be used to compensate for the possible temporal drift and to evaluate the residual uncertainty.

Relative non-linearity error $\delta x(\lambda)$ for the spectrum $S_2(n)$ is:

$$\delta x(\lambda) = \frac{S_2(n) - S_{1,2}(n)}{S_{1,2}(n)} \tag{10}$$

The spectrum $\delta x(\lambda)$ is related with the spectrum $S_2(n)$ of the radiation source. From the analysis of non-linearity data obtained by using the two-spectra formula (9) from the suitable measured calibration data, it became evident that non-linearity errors scaled to the full-range value $\delta x_{max}(\lambda)$ of different radiance sensors behave in a closely similar way [10]. This behaviour serves as a basis for derivation of non-linearity correction applicable to an arbitrary single spectrum and can also be used for outdoor measurements.

$$\delta x_{max}(\lambda) = \frac{S_{max}}{S_{1,2}} \delta x(\lambda) = \frac{2^{16}\mathrm{DN}}{S_{1,2}} \delta x(\lambda). \tag{11}$$

As suggested in [37] [38] and [2], for instrument-related characterisation the non-linearity correction coefficient $\alpha(\lambda)$ shall be used. Coefficient $\alpha(\lambda)$ can be calculated as:

$$\alpha(\lambda) = \frac{\delta x(\lambda)}{S_{1,2}(n)} \tag{12}$$

Relative non-linearity correction for the full range signal $\delta x_{max}(\lambda)$ is related with the coefficient $\alpha(\lambda)$ by simple formula

$$\delta x_{max}(\lambda) = 2^{16}\mathrm{DN}\ \frac{[\alpha(\lambda)]}{\mathrm{DN}} = 2^{16}[\alpha(\lambda)], \tag{13}$$

where $[\alpha(\lambda)]$ is the numerical value of $\alpha(\lambda)$, and constant 2^{16}DN is the saturation value (the largest possible measured DN value) of the RAMSES, HyperOCR or DALEC sensor.

Non-linearity errors are proportional to the integration time used; coefficient $\alpha(\lambda)$ is an instrument-specific parameter, which does not depend on the shape of the initial spectra used for its determination. Nevertheless, coefficient $\alpha(\lambda)$ curves determined from data with shorter integration times have clearly larger noise levels. The effective determination range of $\alpha(\lambda)$ is also smaller than the range where the relative errors can be reasonably determined.

The formulas (9) to (12) have been thoroughly tested on the RAMSES and HyperOCR calibration data. Expression (9) is effective in the range of (400…800) nm for correcting non-linearity, mostly better than 0.2 %. The coefficient $\alpha(\lambda)$ is applicable in a somewhat smaller range with larger uncertainty of the non-linearity correction estimated. Coefficient $\alpha(\lambda)$ obtained from data with different integration times agrees reasonably well with the results of Talone and Zibordi, 2018, based on a different method (inverse-square law describing the irradiance level created by the lamp as a function of the distance between the radiometer and the lamp at a fixed integration time setting).

A relatively simple method for nonlinearity characterization is suggested, where a spectrum of a stable light source is repeatedly measured at the fixed distance with the array spectroradiometer under characterization while varying the integration time to reach different digital count levels of the signal. Only small extra efforts are required for the realization of this method using the same setup as for the irradiance or radiance calibration (6.2, 6.3). The method is valid if the errors of the integration time itself can be neglected. The method is based on the experimental findings of the FRM4SOC project and is validated for RAMSES and HyperOCR radiometers. The applicability to DALEC is under investigation. However, all other methods for nonlinearity characterization are acceptable that are adopted and validated by cal/char laboratories for the non-linearity characterisation.

The reported parameters are listed in Annex A.

7.7. Determination of the dark signal

Radiometers usually have a non-null output called dark signal without any input flux at the entrance optics [2]. Dark signal is caused by the photodetector dark current and additional contributions such as the electronic offset and varies largely with temperature and integration time. Due to varying conditions, frequent measurements of the dark signal is indispensable. The optimal way during both the characterization and the field measurements is to measure the dark signal and the illuminated signal with equal integration times and timely as close as possible to minimize internal temperature drifts between these measurements.

The dark-signal characterisation is performed with the entrance optics closed. The radiometer's output signal is measured as a function of temperature and integration time, and it is strongly advisable to record dark signal always at the shortest and longest integration times available for the instrument. Determination of the dark signal as a function of temperature can be performed simultaneously/in parallel with the determination of the thermal coefficients as described in paragraph 8.8. The reported parameters are listed in Annex A.

7.8. Determination of the thermal sensitivity

For determination of the thermal coefficients, the radiometer must be inserted into a thermally controlled environment. Although any climate chamber with an optical window might be suitable, the OC radiometers can often (RAMSES, HyperOCR – not the case for DALEC, see below) be submersed into the liquid tank, providing much better thermal contact as thermal relaxation times in air can exceed hours. The proposed tank construction is similar to the system used in [39] and is shown in *Figure 7-10*, and the measurement setup in *Figure 7-11*. The characterisation setup with a lamp (in the case of irradiance sensor) or a lamp-plaque or lamp-sphere (in the case of radiance sensors) is alike the corresponding radiometric calibration setups. The crucial parameter of the light source is temporal stability, while the absolute irradiance/radiance output is not that important. The intensity of the light source shall be sufficient to support measurements with selected integration times. The possible light sources include FEL lamps, smaller QTH lamps with radiometric power supplies, an integrating sphere with an integrated QTH lamp etc. The lamps must be seasoned and their output monitored during the measurements for sufficient stability. The alignment is not critical, except for blocking the ambient light. The tank is equipped with (calibrated) temperature sensor TSYS01. A computer controls the whole measurement process, namely setting the temperature, recording the temperature, monitoring signals and acquiring spectra. The water in the tank is circulated by a Julabo FL300 cooler. The temperature set-points were +5 °C, +10 °C, +20 °C, +30 °C and +40 °C. At least two scans shall be performed for each spectrometer, with temperature ramp up and down, respectively.

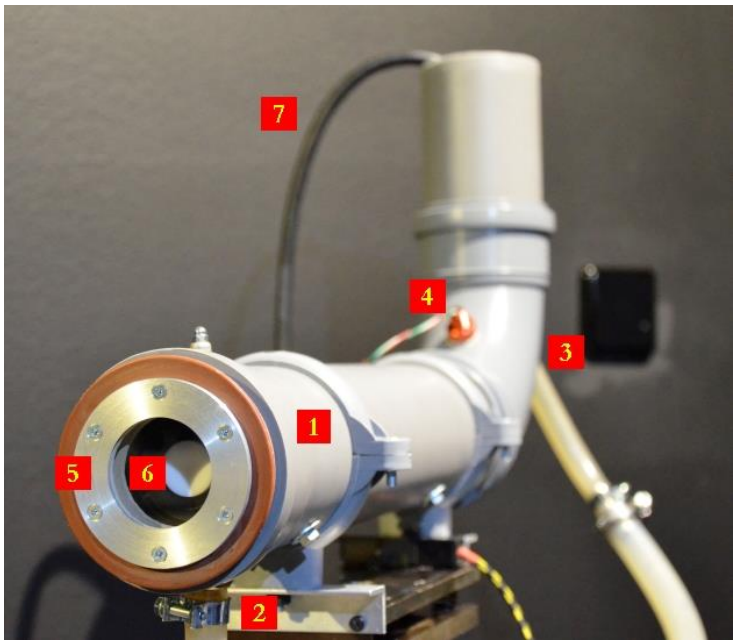

Figure 7-10. Construction of the liquid tank. 1 - tube; 2 - water inlet port; 3 – water outlet port; 4 - temperature sensor; 5 - front window holder; 6 - radiometer; 7 - radiometer cable.

To assess thermal hysteresis, temperature ramps up and down should be used with the same set-points. The temperature field inside the radiometer, affecting the dark signal and radiometric responsivity, has a complex behavior dependent on various components with different thermal relaxation time constants. Moreover, the thermal state of internal electronics depends on the acquisition mode. For unbiased measurements, the radiometer must be switched on and acquire spectra for at least 20 minutes before taking actual measurements at each set-

point. Based on the experience from UT, a 45-60 min relaxation time is needed after reaching the set-point, yielding the full measurement time up to 10 hours.

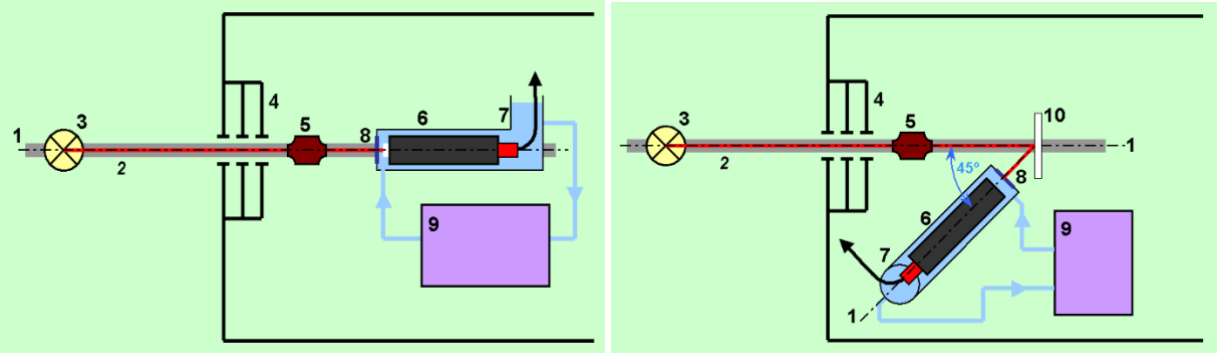

Figure 7-11. Measurement setup for radiometers with cylindrical shape and water-tight housing, TriOS-RAMSES and SeaBird-HyperOCR, for the cases of irradiance (left pane) and radiance (right pane). 1 – optical axis; 2 - rail; 3 – FEL lamp; 4 - baffles; 5 – alignment laser; 6 – radiometer; 7 – thermally controlled tank; 8 – window; 9 – recirculating cooler; 10 – reflectance plaque.

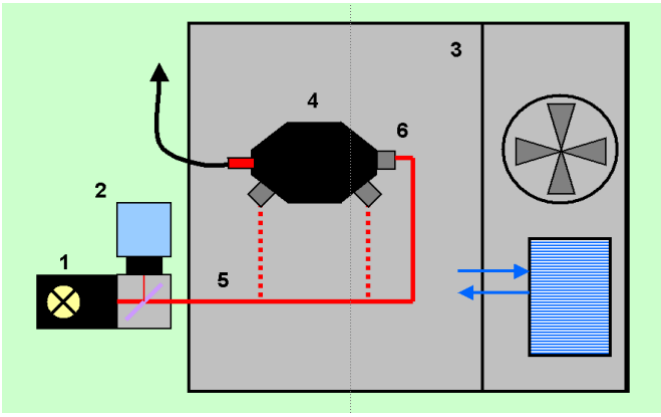

Figure 7-12. Measurement setup for DALEC. 1 – AvaLight-HAL light source; 2 - stability monitor; 3 – WKL-64/40 climate chamber; 4 - DALEC; 5 – optical fiber; 6 – fiber adapter.

In the case of tank measurements, it is advisable to heat up the tank to the highest temperature set-point and, before final alignments, ensure that there are no bubbles on the tank and radiometer windows. At low temperatures (+5, +10) °C, the outer surface of the tank (or climate chamber) window should be checked for possible condensation, depending on the lab's air humidity. Due to the long waiting times between set-points and arbitrary short acquisition time, the thermal measurements can be combined with various characterisations. For example, wavelengths scale (by using lasers or pen-ray lamps) and linearity. The measurement sequence must follow the guidelines given in Section 7.6. Acquisition with different integration times is encouraged, and indeed, dark signal with different integration times, including the longest and shortest available, should be recorded.

The temperature coefficients of DALEC can be measured in a climate chamber such as Weiss WKL64/40. The light can be fed to the radiometric inputs by using fiber-coupled adapters (in Tartu Observatory, the AvaLight-HAL light source was placed externally) and must be monitored for temporal stability (*Figure 7-12*). In the case of DALEC, fast temperature sweeps are possible due to the good coupling between the internal temperature sensors and the linear detectors. Up and down temperature ramps are needed to evaluate the hysteresis (lag between the temperature reading and optical signal) and the corresponding uncertainty contribution.

Data processing must include the following steps (for each pixel):

1) subtracting the dark signal from the closest shutter measurement.
2) finding the slope and intercept of the linear regression between the signal and temperature.
3) combining data from two scans.
4) evaluating uncertainty of the slope.

The reported parameters are listed in Annex A.

7.9. Determination of the polarisation sensitivity

For the characterisation of the polarisation sensitivity of a radiance sensor, a linearly polarised source is needed [40]. The source can be created by using a non-polarised radiance source (an integrating sphere or lamp-plaque setup) and a linear polariser. The setup for polarisation sensitivity measurement is shown in *Figure 7-13*. The sensor azimuth angle shall be defined in the same way as for angular measurements. See *Figure 7-6* in section 7.4. For DALEC, a specialized adapter is needed.

The polarisation sensitivity can be determined by incrementally rotating a linear polariser positioned between a non-polarised source and the entrance optics of the radiometer. The resulting polarisation sensitivity, in percent, can then be expressed as

$$P(\lambda) = 100\frac{DN_M(\lambda) - DN_m(\lambda)}{DN_M(\lambda) + DN_m(\lambda)}, \tag{14}$$

where $DN_m(\lambda)$ and $DN_M(\lambda)$ indicate the minimum and maximum values recorded while rotating the polariser and corrected for the ambient and the dark signals.

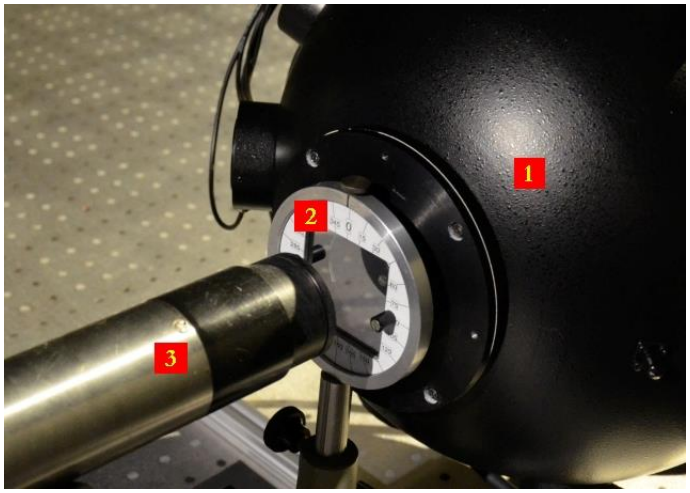

Figure 7-13. Setup for polarisation sensitivity measurement. 1 - integrating sphere with QTH source Bentham ULS300, 2 - 50x50 mm wire-grid polariser in holder, 3 – radiometer.

The considerations are as follows. (I) The higher the extinction ratio of the polarised light, the closer is (14) to the true polarisation sensitivity of the radiometer. The integrating sphere is considered an ideally depolarised source. The extinction ratio of the polariser can be experimentally measured by using, for example, a linearly polarised HeNe laser and photodetector with a wide enough linearity range. The extinction ratios better than 1000:1 in the required wavelength range are sufficient. (II) Only a few per cent deviation of the radiometer's output signal around its average value is expected when rotating the polariser. The parasitic reflection from the polariser holder etc., can significantly distort the measurement results. For that reason, a holder (*Figure 7-13*) with thin edges is recommended. (III) Thermal effects can distort the results when not handled properly. As in the case of linearity (7.6) and thermal characterisations (7.8) the effect can be reduced by careful choice of the measurement sequence. Acquiring (approx. 10 readings) at each set angle should be immediately followed by acquiring the reference signal

at 0°. This approach helps to reduce the drifting source effects as well. The source must be logged and monitored whenever the drift is expected to exceed ±0.1%. The radiometer's integration time shall be fixed. The lamp and the radiometer shall be switched on at least 10 min before the characterisation measurements while the radiometer is constantly acquiring with the probed integration time.

It is proposed to determine the polarisation sensitivity and the azimuthal angle of the maximum responsivity with respect to φ=0° (*Figure 7-6*) covering at least 360°. At least two full periods of responsivity change per full rotation of the polariser should be measured. Covering the full rotation helps to discover possible additional oscillations caused by parasitic reflections into the radiometer's FOV.

The radiometer signal at each set angle is then divided by the signal from the following 0° measurement (all the calculations are spectral, i.e. performed for every pixel). One should be able to approximate the signal vs angle by *signal=A+B*sin(angle+C)*, where A is the unaffected signal, B the amplitude of the azimuthally oscillating signal and C the offset phase. To validate the polarisation sensitivity characterisation, the radiometer can be turned around its optical axis by a known azimuth angle D and the measurement repeated. Parameter B should preserve its value while parameter C should reflect the rotation of the radiometer C → C+D.

The reported parameters are listed in Annex A.

7.10. Determination of the temporal response

To be updated in the following versions of this document.

7.11. Determination of the wavelength scale

The wavelength scale of the typical OC spectroradiometer is given as a function of pixel number n. The function $\lambda(n)$ is typically fitted by polynomials of third to sixth order.

For calibration of the wavelength scale, fixed narrow-band sources (lasers, pen-ray lamps, certified sharp absorption line filters or tuned narrow-band sources such as monochromators and tunable lasers) with known wavelength reference values can be used. In specification, wavelength accuracy of TriOS RAMSES and Seabird's HyperOCR radiometers is stated to be within ±0.3 nm. Therefore, the characterisation setup must provide reference values with smaller or at least with the same uncertainty.

The use of tunable source (scanning monochromator) is described in section 7.1. These measurements can be performed under computer control during stray light characterisation, and then all the pixels of the radiometer will be individually covered. The monochromator must provide accuracy within ±0.3 nm, and uncertainty arising from the determination of the central wavelength (CWL) position for each pixel should also be considered.

Many fixed wavelength sources, like gas lasers (HeNe, Cd) and low-pressure discharge lamps (Ar, Ne, Ag, Kr etc.), are widely used. Most non-stabilised solid-state lasers are not suitable due to the high drift. In the case of fixed-wavelength sources, the emission lines do not coincide with the pixel CWL-s and some interpolation technique should be used. Moreover, as in the case of discharge lamps, spectral lines up to tens of nanometers apart affect the signal of a given pixel, so a weighted sum of several source lines must be considered.

For the determination of the wavelength scale as a function of temperature, Kr-lamp spectra must be recorded for all radiometers subject to cal/char procedure maintaining radiometer at different temperatures in the range from 5 °C to 40 °C. By using these Kr-lamp spectra, the accuracy of the wavelength scale as a function of temperature can be characterised at different wavelengths and at different temperatures. Resolution of radiometers defined as the full width at half maximum (FWHM) of a bandwidth is about $\Delta\lambda_{FWHM} \approx 10$ nm, usually, more than one Kr line will contribute to joint lines recorded by the radiometer. Therefore, all used reference lines λ_{ref} (e.g. those listed in Table 7-1) must be calculated from two suitably-located neighbouring Kr lines λ_1 and λ_2 accounting for their weights w_1 and w_2. Wavelengths and weights of the Kr lines can be obtained from [41]. An example showing the determination of central wavelengths for different temperatures is given in *Figure 7-14*.

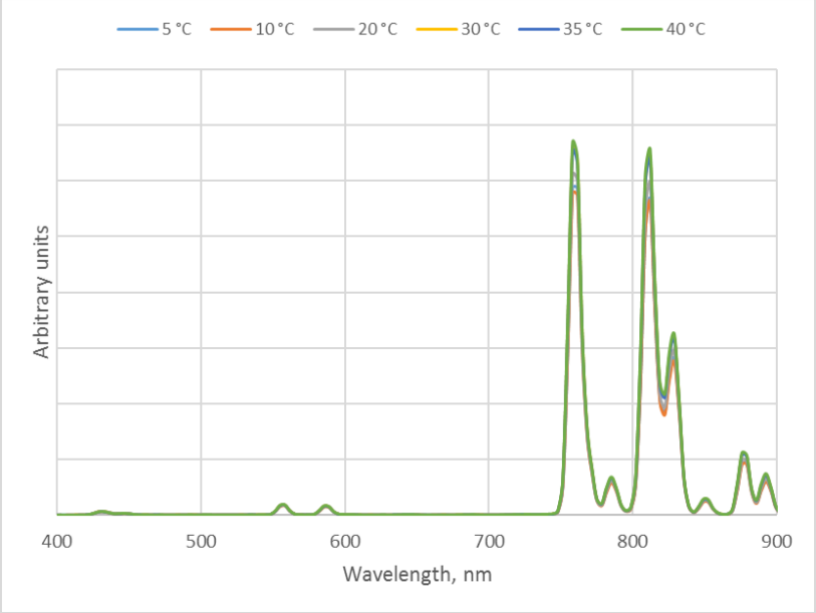

Figure 7-14. Six Kr-lamp spectra as a function of temperature.

Table 7-1. Central wavelength of the reference lines calculated from two neighbouring Kr lines, as obtained in Tartu Observatory.

W	λ1	λ2	w1	w2	w1+w2	λref
Ref1	556.22	557.02	34	163	197	556.88
Ref2	758.74	760.15	1052	3905	4957	759.85
Ref3	810.43	811.29	871	3887	4758	811.13

7.12. Determination of the signal-to-noise ratio

The signal-to-noise ratio *SNR* is determined as the ratio of an averaged signal S_E (dark subtracted) to the standard deviation of a single measurement accounting for the scattering of both light and dark signal.

$$SNR = \frac{S_E}{\sqrt{s_{light}^2 + s_{dark}^2}}, \tag{15}$$

where s_{light} is the standard deviation of the signal distribution and s_{dark} the standard deviation of the dark. Single measurement's distribution is chosen as a reference to make the *SNR* estimates of different radiometers more easily comparable.

Determination of the signal-to-noise ratio as a function of temperature can be performed simultaneously/in parallel with determination of the thermal coefficients as described in section 7.8.

For determination of the signal-to-noise ratio, any stable light source can be used, but sources with spectral distribution close to the natural radiation measured in field are preferred.

The pixels/channels of the radiometer are considered as equivalent, thus the *SNR* dependence on the absolute signal value (presented as ratio to the saturation level) is suitable for describing performance of a particular radiometer for some measurement, presenting a dependence:

$$SNR(S_{rel}) = f\left(\frac{S_{DN}}{DN_{max}}\right) = f(S_{rel}), \quad (16)$$

where S_{DN} is the signal level in digital numbers and DN_{max} denotes the signal saturation level. with *SNR* values re-calculated to the saturation level of the sensor; at this level, maximum values of signal-to-noise ratio for the sensor can be expected.

To get reliable *SNR* values, the drift in recorded time series should be no more than 10% of the standard deviation. In order to ensure that, the source and the radiometer should be switched on and stabilised in the working conditions (i.e. the radiometer acquiring spectra at the selected integration time) for at least 20 min before the actual characterisation measurement, see section 7.8. The reported parameters are listed in Annex A.

8. Gaps in characterisation guidelines

All the characterisation methods and procedures described herein can be fine-tuned to be applied on wider spectral ranges and better signal-to-noise ratios-. Characterisation of parameters that need building of a new measurement facility can be realised only by means of dedicated projects and/or work packages. Major gaps in cal/char procedures at UT are listed in Table 8-1.

Table 8-1. List of parameters needing development of characterisation setups and procedures at UT.

Parameter	Characterisations needing development
Immersion factors	Development started at UT in 2025
Accuracy of integration times	Achievable in future projects
Temporal response	Achievable in future projects
Pressure effects	Achievable in future projects

Correcting procedures of the field results for the several effects like polarisation sensitivity, angular response, straylight errors etc. need further investigation, see Table 8-2.

Table 8-2. List of parameters needing the specific correction procedures to be established and validated.

Parameter	Improvements needed for correction procedures
Stray light and out-of-band response	SNR and dynamic range
Non-linearity	SNR for 350 nm to 450 nm spectral range
Polarisation sensitivity	Establishment and validation of correction procedure
Angular response	Validation of correction procedure

Contrary to the case of absolute responsivity [42], validation of characterisation results through a special laboratory comparison exercise was yet not done for the considered hyperspectral OCR classes. Arranging such a comparison is challenging as routine characterisations of OCRs are done only by a few laboratories. Characterisation comparisons likely should be organised separately for each parameter, and in each comparison only few participants can be involved.

As concluded from the laboratory comparison exercise [42] (D-13), the needs for further study to improve the current document are at least the following:

1. Direct testing of the accuracy of the integration time setting. The laboratory cal/char inter-comparison exercise revealed that at different laboratories the integration time used for the radiance calibration was up to 32 times different. Such large differences entail the need to determine the accuracy of the entire integration timescale, currently not solved in the FRM4SOC Phase 2. For RAMSES and HyperOCR radiometers, twelve settings with values from 4 ms, 8 ms, 16 ms, . . . to 8.192 s are possible. The accuracy

of the whole integration times scale needs direct comparison with a reference instrument. Tartu Observatory (TO) proposes an experiment with a tunable source (such as ULS300 Variable Radiance Uniform Light Source of Bentham) and a precision monitor detector. The source radiance will be tuned to reach equal readings of the radiance device under test (DUT) at different integration times (to avoid radiometric nonlinearity effects) while the exact level is determined by the reference detector at fixed wavelengths.

2. Optimization of conditions for radiance calibration:

   a) **Distance between the lamp and plaque.** The shortest distance is often determined by the physical dimensions of the radiometer. Longer distances improve the uniformity of the light field but reduce radiance levels. The optimal distance likely is 0.5...1 m, depending also on the standard calibration distance of the used lamp. Scaling of the irradiance for different distances needs attention too. TO proposes the use of a reference detector, because using the inverse square law might introduce bigger uncertainties.

   b) **Distance between the plaque and the radiometer.** Although investigated before [43], we did not find clear instructions about choosing the optimal distance between the plaque/sphere and the radiance sensor. There are at least two effects depending on this distance: the back reflection from the radiometer (up to 0.5 %, increasing at shorter distances and applicable to the plaque and the sphere setups) and the vignetting of the light field (increasing together with the distance, applicable to the plaque setup).

   c) The sphere sources used by two participating laboratories show sharp cutoffs below 400 nm. This is likely due to the UV-protected QTH bulbs used with these spheres. The weak UV signal raises the question of whether these sources should be used for NASA's new Earth-observing mission PACE. Additionally, it increases significantly the magnitude of the straylight correction and its related uncertainty contribution during calibration. A source with uncoated QTH bulbs is preferred.

9. Calibration and re-characterisation routine

The calibration and characterisation priority list in Table 9-1 is based on cal/char results of a set of more than 40 hyperspectral field radiometers of the two most common OCR instrument models used for FRM [44], [45]. The table is loosely based on the more formal requirement list as inherited from IOCCG 2019 and available in [2]. Column "Scope" represents current FRM4SOC understanding of the applicability of the class-based properties vs. the individual characterization. In all cases, uncertainty of the measurement results, such as the water leaving radiance and the remote sensing reflectance, is minimized when using individual characterization data. Parameters in Table 9-1 are arranged according to the expected impact on the measurement uncertainty, in descending order of preference. The actual impact is a complicated function of characterization results and field conditions and can only be quantified via full processing of the data. Such analysis could be done applying the functionality of HyperCP [46].

Table 9-1. Priority list for individual OCR calibration/characterisation and the re-characterisation schedule.

Priority	Parameter	Scope	Re-cal/char need	Comments
First	Absolute calibration for radiometric responsivity	individual	1 year, and after each repair or physical shock	Mandatory at least once per year. Ideally, before and after major field campaigns.
First	Radiometric non-linearity	individual/class-specific	during radiometric calibration and after modification of spectrometer module and front-end electronics	A little additional effort from the side of calibration labs is anticipated by following the guidelines in the current document. If raw calibration data at two different integration times is available, the non-linearity coefficient can be evaluated.
First	Angular response(irradiance)	individual	after modification of fore-optics	Cosine error is fully affecting the uncertainty of the remote sensing reflectance. Individual characterization is highly recommended as the spread within the class is high.
Second	Thermal responsivity	individual/class-specific	after modification of fore-optics, spectrometer module and front-end electronics	Without correction a few percents uncertainty contribution is expected in NIR spectral region. Class-specific data is available, but individual characterization reduces the measurement uncertainty significantly.
Second	Stray light and out of band response	individual	after modification of fore-optics or spectrometer module	Uncertainty contribution of several percents in UV spectral region can be expected if correction is not applied. Class-specific characteristics are available, but individual is preferable.
Second	Angular response (radiance)	individual/class-specific	after modification of fore-optics	No serious deviations observed during FRM4SOC. Negligible impact on the final uncertainties expected.
Second	Polarisation sensitivity	class-specific	after modification of fore-optics or spectrometer module	Only needed for radiance sensors. In the worst case, bias of the remote sensing reflectance can reach a few percents in NIR. Characterization is recommended to collect data for future research.

Table 9-1. (continued) Priority list for individual OCR calibration/characterisation and the re-characterisation schedule.

Priority	Parameter	Scope	Re-cal/char need	Comments
Third	Wavelength scale	individual	if in doubt	Based on FRM4SOC, wavelength scales of RAMSES, HyperOCR and DALEC were within specification for the full temperature range. Can be re-characterized by users with the help of a line source (gas discharge lamps, gas lasers).
Third	Dark signal	individual	1 year, and after modification of front-end electronics	No calibration service needed: can be characterized by users.
Third	Signal-to-noise ratio	class-specific	1 year and after modification of front-end electronics	No calibration service needed: can be characterized by users with the help of a stable light source.
Third	Long term stability	individual	Re-evaluation after every calibration	To be analyzed by users based on available calibration data.
Depending on use	Immersion factor (irradiance)	individual	after modification of fore-optics	Only needed for in-water radiometry. Not characterized during FRM4SOC.
Depending on use	Angular response in water (irradiance)	individual	after modification of fore-optics	Only needed for in-water radiometry. Not characterized during FRM4SOC.
Depending on use	Immersion factor (radiance)	class-specific	after modification of fore-optics	Only needed for in-water radiometry. Strong class-specific behaviour can be expected.
Depending on use	Angular response in water (radiance)	individual, class-specific	after modification of fore-optics	Only needed for in-water radiometry. Strong class-specific behaviour can be expected.
Depending on use	Pressure effects	TBD	after modification of fore-optics	Only needed for in-water radiometry.
	Accuracy of integration times	class-specific	after modification of firmware	Indirectly estimated during FRM4SOC. Avoid 4 ms integration time (RAMSES, HyperOCR). Add 4 ms to the reported integration time (DALEC).
	Temporal response	class-specific	after modification of front-end electronics or firmware	Not characterized during FRM4SOC, further investigation expected.

10. Conclusions

Several Round-Robin Experiments arranged during the last decades for testing, validation of performance, and calibration and characterisation activities of OCR instruments demonstrate clearly that firm traceability of measurements to the SI units is fundamental. Calibration and/or characterisation of measurement instruments at an NMI or at an accredited laboratory is preferred, but accessibility to services is limited and obtaining needed cal/char results may be rather time-consuming and expensive. Therefore, more service providers would be desirable. This document aimed at further expanding the IOCCG harmonised guidelines for secondary cal/char laboratories [2], specializing those models belonging to the FRMOCnet as established within the FRM4SOC Phase 2 Project [47] The guidelines were prepared by Tartu Observatory under the supervision of NPL and intend to establish a shared and common standard at the cal/char laboratory level, ensuring full adoption of traceability requirements for the radiance/irradiance lab standards, measurement results and uncertainties. Differences in hard- and software of OCRs make the characterisation procedures model-sensitive and hinder the harmonisation of the guidelines. In addition, the list of parameters needing characterisation often depends on the model subject to characterisation. Therefore, this document focused on two of the most common models used for FRM: TriOS RAMSES and Sea-Bird's HyperOCR (radiance and irradiance) hyperspectral radiometers. The case of IMO/DALEC was also partially assessed.

Complete calibration and characterisation and regular re-calibration of OCRs is needed due to significant responsivity drift of sensors, due to possible bias of single instruments from ideal realization of specification values, and for accounting environmental factors, which may affect the results. Therefore, any field radiometer used for the satellite ocean color validation should have a documented history of SI traceable calibrations and characterisations. Spectral radiometric responsivity should be preferably determined before and after each major field deployment, but at least regularly once a year. The general scheme for the complete cal/char presented in these guidelines is mostly in close agreement with previous documents - IOCGG protocols [2] and to the strategy plan D11 [12] - which already give rather detailed guidelines for many characterisations. Some characterisation methods (such as immersion factors) have been taken from [2] without changes as no further assessments were done in the frame of FRM4SOC-2. However, new approaches and elements have been described for most cases.

The spectral responsivity of a radiometer is usually calibrated by measuring a known radiation source aligned at a specified distance. The procedures are well established and validated, but unfortunately, there can be significant differences between the calibration and later field use, as regards of operating temperature, angular variation of the light field (especially for irradiance sensors), the intensity of the measured radiation, spectral variation of the target etc. Each of these factors may interact with individual instrument properties when used in the field, and estimation of such uncertainties requires instrument characterisation in addition to the absolute radiometric calibration [2], [10], [11]. Furthermore, most calibrations and characterisations are performed in strictly controlled stable conditions, but field measurements are often in variable or strongly varying conditions. Regarding the results of dynamic characterisations described in [44], [45], some dynamic characterisations would be indispensable to achieve firm SI traceability.

An important finding is that the internal thermal properties of the radiometers may affect cal/char results significantly. Both the dark signal and the radiometric responsivity have significant dependence on temperature, especially above 20 °C and with long (>1 s) integration times. Change of the radiometric response due to the self-heating in stable lab conditions can distort the calibration and characterisation results as small deviations in spectra due to polarization and/or angular effects can be of the same magnitude as the responsivity change of the radiometer due to changes in temperature. The radiometer's response will drift with the varying internal temperature due to self-heating, in turn dependent on the data acquisition mode. Internal temperature can rise, but it can also drop if the previous state of the sensor caused more self-heating. Due to internal self-heating, achieving good reproducibility of the characterisation results may be rather difficult. Because of this, regular recording of specified reference signal between routine characterisation steps is strongly advisable.

Temperature of radiometer's optical sensor is a key parameter for application of many corrections as many calibration and characterisation results depend on temperature. Due to long thermal relaxation times, as many temperature-depending parameters as possible shall be measured right after thermal relaxation or using the defined measurement sequence. The list of parameters includes

- responsivity of a radiometer.
- dark signal.
- non-linear response.
- signal-to-noise ratio.
- accuracy of the wavelength scale.

Some of these dependencies are critical, and some are less important, but for a smooth full characterisation procedure, the measurement sequence and data format of recorded time series shall be purpose-based and well designed.

Specifying the sensor's temperature is a critical issue, especially for sensors without internal temperature sensor installed in the close vicinity of the optical sensor. To some extent, using the dark signal to determine the temperature of the optical sensor may be helpful. However, calibration of internal sensors or validation of calculated temperature values still is problematic. In one case, if present, the internal temperature sensor cannot be taken out of the radiometer for calibration. In the opposite case, there is no effective reference to validate the internal temperatures inferred from proxies such as the dark signal.

Traceability requirements for calibration and for characterisation are usually different. Firm SI traceability with reasonably small uncertainty for calibration standards is very important. For most characterisations, relative deviation due to some influence quantity is determined, and thus, good stability of measurement instruments is sufficient. Nevertheless, several other properties and requirements shall be fulfilled for other characterisations, such as

- temporal stability.
- spectral distribution.
- size of the source (point source).
- quality of collimated beam (spatial distribution, parallelism).

Angle characteristics of TriOS RAMSES irradiance sensors are often strongly non-symmetrical and thus, depend on the azimuth angle used for measurements. This circumstance also makes the further use of characterisation results much more difficult: the azimuth angle must be specified during characterisation and specified and accounted for during the later use.

A major bottleneck is limited spectral range of characterisation results. Intensity of the UV spectrum of FEL lamp is relatively weak and therefore, the uncertainty of cal/char results too large, and useful spectral range is limited. Therefore, a new radiation source is urgently needed for characterisations.

Development and testing of new methods and procedures could also be calibration and characterization of spectroradiometers using tunable lasers [48], [49], [50], [51]. However, such improvement needs costly new equipment and is very time and resource consuming.

As an alternative to the use of FEL lamps for characterisation, the pixel-by-pixel characterisation method by using a monochromatic adjustable source can be suggested. At TO, the method has been used for the stray light and for the non-linearity characterisations. However, such method is much more time-consuming if the full spectral range is measured pixel by pixel. But the method may be quite effective if applied for characterisation of a limited number of selected pixels in the more uncertain spectral bands to be used for validation of the full-spectral characterisations.

For some properties of radiometers, dynamic tests are indispensable. Only thanks to dynamic temperature scanning the anomalous behaviour of cosine collectors of HyperOCR sensors has been revealed. Another important feature detected during dynamic tests is the hysteresis of optical response and its dependence on a particular sensor used for temperature determination. Such an effect may significantly contribute to the uncertainty of field results. To account for dynamic effects during field measurements, the best solution would be to have two temperature sensors installed in each radiometer: one sensor in close vicinity to the optical sensor and another on the surface of the radiometer. Differences between sensors will show the speed of temperature variation and give input for dynamic influences.

The FidRadDB (”Fiducial Radiometer” Data Base) [52] is a database containing information on radiometric calibration and characterisations done on field Ocean Colour radiometers. Development of the OCDB FidRadDB database started in April 2021. Since then, 12 class-based characterisation files for HYPEROCR and RAMSES radiometer were created and are stored in the FidRadDB database. For major properties of OCRs, class-based characteristics (arithmetic mean together with uncertainties covering the individual spread) were derived for nonlinearity coefficients, temperature coefficients, straylight matrices, angular response, and polarization sensitivity. The corrections are applicable in the range from 500 nm to 800 nm, but in the UV and NIR spectral regions the low signal-to-noise ratio can strongly affect the characterisation. To make effective correcting possible in the full spectral range, a reduction of the characterization noise in the beginning and end part of the range is

needed, or a metrologically supported criterion for discriminating small corrections with uncertainties much larger than the corrections itself.

For the assessment of stray light, improved straylight matrices and optimization of correction methods (applicable to the laboratory and field measurements) are needed. There are currently two alternative methods for straylight correction: the iteration method and the matrix inversion method. The iteration method tends to improve the spectral resolution but adds random noise to the corrected spectrum. The matrix inversion method completely ignores the spectral effects within the in-band region (width of few pixels). The latter can introduce systematic biases when deriving OC products based on band ratios. Extensive testing with different sensors and spectral shapes is needed. Noise of straylight matrices should be reduced and screening of applicability regions introduced.

11. References

[1] J. L. Mueller *et al.*, "Ocean Optics Protocols For Satellite Ocean Color Sensor Validation, Revision 4. Volume III: Radiometric Measurements and Data Analysis Protocols.," 2003, doi: http://dx.doi.org/10.25607/OBP-62.

[2] G. Zibordi, K. Voss, B. C. Johnson, and J. L. Mueller, "IOCCG Protocol Series (2019). Protocols for Satellite Ocean Colour Data Validation: In Situ Optical Radiometry. Zibordi, G., Voss, K. J., Johnson, B. C. and Mueller, J. L. IOCCG Ocean Optics and Biogeochemistry Protocols for Satellite Ocean Colour Sensor Validation, Volume 3.0," IOCCG, Dartmouth, NS, Canada, 2019. doi: http://dx.doi.org/10.25607/OBP-691.

[3] "JCGM 200:2008: International Vocabulary of Metrology - Basic and General Concepts and Associated Terms (VIM)." BIPM, Aug. 2011.

[4] "CIPM (1999) Mutual Recognition of National Measurement Standards and of Calibration and Measurement Certificates Issued by National Metrology Institutes." CIPM, 1999.

[5] S. B. Hooker *et al.*, "The Seventh SeaWiFS Intercalibration Round-Robin Experiment (SIRREX-7), TM-2003-206892, vol. 17, NASA Goddard Space Flight Center, Greenbelt," Feb. 2002, Accessed: Feb. 08, 2017. [Online]. Available: http://ntrs.nasa.gov/search.jsp?R=20020045342

[6] L. Ylianttila, R. Visuri, L. Huurto, and K. Jokela, "Evaluation of a Single-monochromator Diode Array Spectroradiometer for Sunbed UV-radiation Measurements¶," *Photochem. Photobiol.*, vol. 81, no. 2, pp. 333–341, 2005, doi: 10.1111/j.1751-1097.2005.tb00192.x.

[7] G. Seckmeyer, "Instruments to Measure Solar Ultraviolet Radiation Part 4: Array Spectroradiometers (lead author: G. Seckmeyer) (WMO/TD No. 1538). 44 pp. November 2010." WMO, 2010.

[8] C. Johnson, H. Yoon, J. P. Rice, and A. C. Parr, "Chapter 1.2 - Principles of Optical Radiometry and Measurement Uncertainty," in *Experimental Methods in the Physical Sciences*, vol. 47, G. Zibordi, C. J. Donlon, and A. C. Parr, Eds., in Optical Radiometry for Ocean Climate Measurements, vol. 47. , Academic Press, 2014, pp. 13–67. doi: 10.1016/B978-0-12-417011-7.00003-9.

[9] S. G. R. Salim, E. R. Woolliams, and N. P. Fox, "Calibration of a Photodiode Array Spectrometer Against the Copper Point," *Int. J. Thermophys.*, vol. 35, no. 3–4, pp. 504–515, May 2014, doi: 10.1007/s10765-014-1609-1.

[10] V. Vabson *et al.*, "Laboratory Intercomparison of Radiometers Used for Satellite Validation in the 400–900 nm Range," *Remote Sens.*, vol. 11, no. 9, p. 1101, Jan. 2019, doi: 10.3390/rs11091101.

[11] V. Vabson *et al.*, "Field Intercomparison of Radiometers Used for Satellite Validation in the 400–900 nm Range," *Remote Sens.*, vol. 11, no. 9, p. 1129, Jan. 2019, doi: 10.3390/rs11091129.

[12] A. Białek, "FRM4SOC2-D11. Strategy plan for the secondary laboratory cal/char inter-comparison exercise and the definition and harmonization of laboratory guidelines." EUMETSAT, Nov. 25, 2021.

[13] TriOS, "RAMSES Technische Spezifikationen," TriOS Mess- und Datentechnik. Accessed: Jan. 31, 2019. [Online]. Available: https://www.trios.de/ramses.html

[14] Sea-Bird Scientific, "Specifications for HyperOCR Radiometer." Accessed: Jan. 31, 2019. [Online]. Available: https://www.seabird.com/hyperspectral-radiometers/hyperocr-radiometer/family?productCategoryId=54627869935

[15] "DALEC | In-situ Marine Optics," In-situ Marine Optics |. Accessed: Jun. 25, 2024. [Online]. Available: https://insitumarineoptics.com/dalec/

[16] Carl Zeiss, "Zeiss Spectrometer Modules Compendium, MMS Family, MMS 1." Accessed: Oct. 06, 2025. [Online]. Available: https://www.google.com/search?q=Carl+Zeiss+MMS1+UV/VIS+Spectrometer&sca_esv=cbb7f6c3823ad055&sxsrf=AE3TifNuNIwo83p05zUyDYGI9dlXpNVjPw:1759743027819&ei=M4zjaLnpMaH9wPAPyaicoQ8&start=10&sa=N&sstk=Af77f_eiJwDmNDtSx_03cwmU8XwDICDgc2qJuBzWMZ3VQtNMbgLFqYBMsXJWeWBgWzoWKTP3wqq1MS4qgghe68S9jfs7QqLWvDs_iA&ved=2ahUKEwj5zsbQoY-QAxWhPhAIHUkUJ_QQ8tMDegQIDxAE&biw=1826&bih=1039&dpr=1

[17] P. Goryl, N. Fox, C. Donlon, and P. Castracane, "Fiducial Reference Measurements (FRMs): What Are They?," *Remote Sens.*, vol. 15, no. 20, p. 5017, Jan. 2023, doi: 10.3390/rs15205017.

[18] "ISO/IEC 17025:2017 General requirements for the competence of testing and calibration laboratories," ISO. Accessed: Aug. 01, 2022. [Online]. Available: https://www.iso.org/cms/render/live/en/sites/isoorg/contents/data/standard/06/69/66912.html

[19] "FRM4SOC-2, FRM Requirements Document for Instrument Manufacturers (RMANU), Deliverable D-27, May 2023, https://frm4soc2.eumetsat.int."

[20] N. Fox and M.-C. Greening, "QA4EO guide: QA4EO-QAEO-GEN-DQK-007, A guide to establishing quantitative evidence of traceability to underpin the Quality Assurance requirements of GEO, QA4EO, V4.0. 27.03.2010."

[21] D. Pissulla *et al.*, "Comparison of atmospheric spectral radiance measurements from five independently calibrated systems," *Photochem. Photobiol. Sci. Off. J. Eur. Photochem. Assoc. Eur. Soc. Photobiol.*, vol. 8, no. 4, pp. 516–527, Apr. 2009, doi: 10.1039/b817018e.
[22] G. Bernhard and G. Seckmeyer, "Uncertainty of measurements of spectral solar UV irradiance," *J. Geophys. Res. Atmospheres*, vol. 104, no. D12, pp. 14321–14345, Jun. 1999, doi: 10.1029/1999JD900180.
[23] C. P. Ball *et al.*, "Effect of polytetrafluoroethylene (PTFE) phase transition at 19 °C on the use of Spectralon as a reference standard for reflectance," *Appl. Opt.*, vol. 52, no. 20, pp. 4806–4812, Jul. 2013, doi: 10.1364/AO.52.004806.
[24] B. C. Johnson *et al.*, "The Fifth SeaWiFS Intercalibration Round-Robin Experiment (SIRREX-S), July 1996," vol. 7, Oct. 1999, Accessed: Apr. 12, 2020. [Online]. Available: https://www.nist.gov/publications/fifth-seawifs-intercalibration-round-robin-experiment-sirrex-s-july-1996
[25] M. E. Feinholz *et al.*, "Stray light correction algorithm for multichannel hyperspectral spectrographs," *Appl. Opt.*, vol. 51, no. 16, pp. 3631–3641, Jun. 2012.
[26] M. Talone, G. Zibordi, I. Ansko, A. C. Banks, and J. Kuusk, "Stray light effects in above-water remote-sensing reflectance from hyperspectral radiometers," *Appl. Opt.*, vol. 55, no. 15, pp. 3966–3977, May 2016, doi: 10.1364/AO.55.003966.
[27] H. Kostkowski, *Reliable Spectroradiometry*. Spectroradiometry Consulting, 1997.
[28] H. Slaper, H. a. J. M. Reinen, M. Blumthaler, M. Huber, and F. Kuik, "Comparing ground-level spectrally resolved solar UV measurements using various instruments: A technique resolving effects of wavelength shift and slit width," *Geophys. Res. Lett.*, vol. 22, no. 20, pp. 2721–2724, Oct. 1995, doi: 10.1029/95GL02824.
[29] S. Nevas, A. Sperling, and B. Oderkerk, "Transferability of stray light corrections among array spectroradiometers," in *AIP Conference Proceedings*, AIP Publishing, May 2013, pp. 821–824. doi: 10.1063/1.4804896.
[30] D. F. Westlake, "Some Problems in the Measurement of Radiation Under Water: A Review," *Photochem. Photobiol.*, vol. 4, no. 5, pp. 849–868, 1965, doi: 10.1111/j.1751-1097.1965.tb07933.x.
[31] G. Zibordi, S. B. Hooker, J. Mueller, and G. Lazin, "Characterization of the Immersion Factor for a Series of In-Water Optical Radiometers," *J. Atmospheric Ocean. Technol.*, vol. 21, no. 3, pp. 501–514, Mar. 2004, doi: 10.1175/1520-0426(2004)021<0501:COTIFF>2.0.CO;2.
[32] G. Zibordi, "Immersion Factor of In-Water Radiance Sensors: Assessment for a Class of Radiometers," *J. Atmospheric Ocean. Technol.*, vol. 23, no. 2, pp. 302–313, Feb. 2006, doi: 10.1175/JTECH1847.1.
[33] G. Zibordi and M. Darecki, "Immersion factors for the RAMSES series of hyper-spectral underwater radiometers," *J. Opt. Pure Appl. Opt.*, vol. 8, no. 3, pp. 252–258, Jan. 2006, doi: 10.1088/1464-4258/8/3/005.
[34] G. Zibordi and P. Sciuto, "Advances in Marine Optics Technology," *JRC Tech. Rep.*, 2022, doi: 10.2760/387681.
[35] M. Talone and G. Zibordi, "Spatial uniformity of the spectral radiance by white LED-based flat-fields," *OSA Contin.*, vol. 3, no. 9, pp. 2501–2511, Sep. 2020, doi: 10.1364/OSAC.394805.
[36] V. Vabson, I. Ansko, R. Vendt, and J. Kuusk, "Technical Report D12: Harmonised cal/char lab guidelines, including lab protocols for FRMOCnet OCR models." EUMETSAT: Darmstadt, Germany, Nov. 2022.
[37] M. Talone and G. Zibordi, "Non-linear response of a class of hyper-spectral radiometers," *Metrologia*, vol. 55, no. 5, pp. 747–758, Sep. 2018, doi: 10.1088/1681-7575/aadd7f.
[38] M. Talone, G. Zibordi, and A. Bialek, "Reduction of non-linearity effects for a class of hyper-spectral radiometers," *Metrologia*, vol. 57, no. 2, p. 025008, Mar. 2020, doi: 10.1088/1681-7575/ab6277.
[39] G. Zibordi, M. Talone, and L. Jankowski, "Response to Temperature of a Class of In Situ Hyperspectral Radiometers," *J. Atmospheric Ocean. Technol.*, vol. 34, no. 8, pp. 1795–1805, Aug. 2017, doi: 10.1175/JTECH-D-17-0048.1.
[40] M. Talone and G. Zibordi, "Polarimetric characteristics of a class of hyperspectral radiometers," *Appl. Opt.*, vol. 55, no. 35, pp. 10092–10104, Dec. 2016, doi: 10.1364/AO.55.010092.
[41] T. Jacksier and R. M. Barnes, "Atomic Emission Spectra of Xenon, Krypton, and Neon: Spectra from 200 to 900 nm by Sealed Inductively Coupled Plasma/Atomic Emission Spectroscopy," *Appl. Spectrosc.*, vol. 48, no. 1, pp. 65–71, Jan. 1994, doi: 10.1366/0003702944027543.
[42] V. Vabson *et al.*, "Laboratory Calibration Comparison of Hyperspectral Ocean Color Radiometers in the Frame of the FRM4SOC Phase 2 Project," *Remote Sens.*, vol. 17, no. 22, p. 3692, Nov. 2025, doi: 10.3390/rs17223692.
[43] A. Białek *et al.*, "Results from Verification of Reference Irradiance and Radiance Sources Laboratory Calibration Experiment Campaign," *Remote Sens.*, Art. no. 5, 2020.
[44] V. Vabson *et al.*, "Complete characterization of ocean color radiometers," *Front. Remote Sens.*, vol. 5, Apr. 2024, doi: 10.3389/frsen.2024.1320454.

[45] V. Vabson, I. Ansko, R. Vendt, and J. Kuusk, "Technical Report D7: Complete characterisation and calibration results for FRMOCnet OCR models and re-characterisation routine: an update." EUMETSAT: Darmstadt, Germany, Nov. 2022.
[46] G. Tilstone *et al.*, "Radiometric field inter-comparison of fiducial reference measurements using an open source community processor," *Opt. Express*, vol. 33, pp. 15756–15781, Apr. 2025, doi: 10.1364/OE.551042.
[47] "EUMETSAT | FRM4SOC Phase-2." Accessed: Nov. 27, 2025. [Online]. Available: https://frm4soc2.eumetsat.int/
[48] S. van den Berg, P. Dekker, G. Otter, M. P. Páscoa, and N. Dijkhuizen, "Calibration of a CubeSat spectroradiometer with a narrow-band widely tunable radiance source," *Appl. Opt.*, vol. 60, no. 7, pp. 1995–2002, Mar. 2021, doi: 10.1364/AO.417467.
[49] M. Schuster, S. Nevas, A. Sperling, and S. Völker, "Spectral calibration of radiometric detectors using tunable laser sources," *Appl. Opt.*, vol. 51, no. 12, pp. 1950–1961, Apr. 2012, doi: 10.1364/AO.51.001950.
[50] J. T. Woodward, P.-S. Shaw, H. W. Yoon, Y. Zong, S. W. Brown, and K. R. Lykke, "Invited Article: Advances in tunable laser-based radiometric calibration applications at the National Institute of Standards and Technology, USA," *Rev. Sci. Instrum.*, vol. 89, no. 9, p. 091301, Sep. 2018, doi: 10.1063/1.5004810.
[51] Y. Zong, P.-S. Shaw, J. P. Rice, and C. C. Miller, "CALIBRATION OF SPECTRORADIOMETERS USING TUNABLE LASERS," in *PROCEEDINGS OF the 29th Quadrennial Session of the CIE*, Washington DC, USA: International Commission on Illumination, CIE, Jun. 2019, pp. 569–574. doi: 10.25039/x46.2019.OP77.
[52] "The FidRadDB database — Copernicus Ocean Colour Database documentation." Accessed: Jan. 14, 2026. [Online]. Available: https://ocdb.eumetsat.int/docs/fidrad-database.html

Annex A. Cal/char data formats compatible with the HyperCP

The FidRadDB ("Fiducial Radiometer" Data Base) [52] is a database containing information on radiometric calibration and characterisations done on field Ocean Colour radiometers. The initial objective of the FidRadDB is to centralise all existing information on cal/char of TriOS and SeaBird radiometers calibrated and characterised at the Tartu Observatory (University of Tartu, Estonia) in the frame on the FRM4SOC-2 project. Future endeavors may include cal/char coefficients obtained in other contexts or for other instruments. To be accepted in the FidRadDB, cal/char files need to be in accordance with the format defined by the Tartu Obstervatory (for more information keep reading below). FidRadDB allows different actions (submitting new files, querying the database, downloading files, etc.).

A0 FidRadDB file naming convention

```
CP_[DEVICE]_[TYPE]_[DATE].txt

[DEVICE]:
       SAM_XXXX       TriOS Ramses, XXXX = Serial number
       SATXXXX        SeaBird/Satlantic HyperOCR, XXXX = Serial number
       DAL_XXXX_YYYYYY       IMO DALEC, XXXX = Serial number, YYYYYY = Module number

[TYPE]:
       RADCAL         Radiometric calibration
       ANGULAR        Angular responsivity
       POLAR          Polarization sensitivity
       STRAY          Inherent straylight
       THERMAL Thermal sensitivity

[DATE]: yyyymmddhhmmss Date and time of calibration/characterization

Example: CP_SAT2073_RADCAL_20250902122025.txt
```

A1 Radiometric calibration coefficients & linearity, lamp and plaque data

```
!FRM4SOC_CP
!RADCAL
# radiometric calibration coefs & linearity, lamp and panel data

# comments start with # (ignored by the processor)
# no empty lines between the parameter signatures in [] and the parameter values
# parameters are case insensitive
# parameters can be inserted in any order, except the first two signatures
# columns are tab- or space-delimited

# file format version
# type(s): string(255)
[VERSION]
0.1

# calibration date yyyy-mm-dd hh:mm:ss
# type(s): string(255)
[CALDATE]
2025-09-02 12:20:25

# calibration lab name
# type(s): string(255)
[CALLAB]
Tartu Observatory
```

```
# calibration lab person to contact
# type(s): string(255)
[USER]
Riho Vendt

# serial number of the calibrated instrument
# type(s): string(255)
# SAM_XXXX: TriOS Ramses, XXXX = Serial number
# SATXXXX: SeaBird/Satlantic HyperOCR, XXXX = Serial number
# DAL_XXXX_YYYYYY: IMO DALEC, XXXX = Serial number, YYYYYY = Module number
# e.g. SAM_8166, SAT0222, DAL_0012_144461
[DEVICE]
SAT2073

# lab temperature (deg Celsius) during cal/char measurements
# type(s): single
[AMBIENT_TEMP]
21.0

# radiometer internal temperature (deg Celsius) during cal/char measurements when available
# optional
# type(s): single
[DEVICE_TEMP]
23.88

# for reference only
# type(s): string(255)
[LAMP_ID]
TO_7

# for reference only
# type(s): string(255)
[PANEL_ID]
SG3151/1

# Correlated color temperature (K)
# type(s): single
[LAMP_CCT]
2977.5

# lamp data (line count is arbitrary)
# wavelength (nm), bandwidth (nm), irradiane (mW/m2/nm), uncertainty (%, k=2)
# type(s): single
[LAMPDATA]
300.00  0.00    1.3608  1.50
310.00  0.00    1.9372  1.50
320.00  0.00    2.6358  1.50
...
980.00  0.00    201.7270        1.20
990.00  0.00    202.1353        1.30
1000.00 0.00    202.4295        1.30
[END_OF_LAMPDATA]

# panel data (line count is arbitrary)
# not mandatory for irradiance sensors
# wavelength (nm), bandwidth (nm), reflectance, uncertainty (%, k=2)
# type(s): single
[PANELDATA]
350.00  0.00    0.9740  1.17
360.00  0.00    0.9820  1.18
370.00  0.00    0.9850  1.18
...
1680.00 0.00    0.9570  0.48
1690.00 0.00    0.9530  0.48
1700.00 0.00    0.9490  0.47
[END_OF_PANELDATA]
```

```
# radiometer data
# pixel no, wavelength (nm), irradiane responsivity (unit depends on the device class),
uncertainty (%, k=2),
# dark1, dark2 (content depends on the instrument class: ignore for HyperOCR and DALEC;
Back_SAM_XXXX.dat data for TriOS), raw1, stdev1, raw2, stdev2
# First row of the column 'responsivity' depends on instrument class (TriOS Ramses - integration
timem index; HyperOCR - integration time (ms)).
# First row of the columns 'raw1' and 'raw2' contains integration time for the given colums.
# type(s): uint8, single, single, single, single, single, single, single, single, single
[CALDATA]
0       305.10  4       0.00    12      0.000000        64      0.00    32      0.00
1       308.37  0.574474        6.49    0.020026        0.027088        160.13  1.04    160.77  2.38
2       311.64  0.597737        6.86    0.020077        0.026742        188.53  1.48    188.07  2.93
3       314.91  0.660105        4.67    0.019895        0.026660        228.83  1.00    229.47  2.26
...
253     1130.18 0.000000        68.74   0.020013        0.026230        -2.27   1.28    -6.03   1.56
254     1133.34 0.000000        733.15  0.020231        0.026084        -3.77   0.81    -1.13   2.72
255     1136.49 0.000000        271.99  0.020603        0.027199        -4.72   0.93    -1.33   1.31
[END_OF_CALDATA]
```

A2 Angular responsivity characterisation files

```
!FRM4SOC_CP
!ANGDATA
# angular responsivity characterization results


# comments start with # (ignored by the processor)

# no empty lines between the parameter signatures in [] and the parameter values

# parameters are case insensitive
# parameters can be inserted in any order, except the first two signatures

# columns are tab- or space-delimited


# file format version
# type(s): string(255)
[VERSION]
0.1

# calibration date yyyy-mm-dd hh:mm:ss
# type(s): string(255)
[CALDATE]
2025-09-02 12:20:25

# calibration lab name
# type(s): string(255)
[CALLAB]
Tartu Observatory

# calibration lab person to contact
# type(s): string(255)
[USER]
Riho Vendt

# serial number of the calibrated instrument
# type(s): string(255)
# SAM_XXXX: TriOS Ramses, XXXX = Serial number
# SATXXXX: SeaBird/Satlantic HyperOCR, XXXX = Serial number
# DAL_XXXX_YYYYYY: IMO DALEC, XXXX = Serial number, YYYYYY = Module number
# e.g. SAM_8166, SAT0222, DAL_0012_144461
[DEVICE]
SAT2073
```

```
# lab temperature (deg Celsius) during cal/char measurements
# type(s): single
[AMBIENT_TEMP]
21.0

# radiometer internal temperature (deg Celsius) during cal/char measurements when available
# optional
# type(s): single
[DEVICE_TEMP]
23.88

# data block contains AZIMUTH_ANGLE, COLUMN_NAMES, COSERROR and UNCERTAINTY (optional) in given
order
# number of data blocks is not limited, to be auto-detected

# scanning azimuth plane
# type(s): single
[AZIMUTH_ANGLE]
0.0

# header row of the following table, containing incident angles (deg)
# type(s): string, string, single ...
[COLUMN_NAMES]
px      wl\angle       -90     -85     -80     ...     80      85      90

# deviation from cosine law (%)
# type(s): uint(8), single, single ...
[COSERROR]
0       303.41  3       3       3       ...     3       3       3
1       306.75  7.62    7.62    -5.44   ...     1.22    22.69   22.69
2       310.09  7.75    7.75    -6.05   ...     -0.68   15.03   15.03
...
253     1130.55 -28.4   -28.4   -4.65   ...     -65.32  -54.42  -54.42
254     1133.63 164.46  164.46  20.22   ...     -108.28 8.94    8.94
255     1136.7  290.89  290.89  92.39   ...     120.93  260.82  260.82
[END_OF_COSERROR]

# header row of the following table, containing incident angles (deg)
# type(s): string, string, single ...
[COLUMN_NAMES]
px      wl\angle       -90     -85     -80     ...     80      85      90

# the same as COSERROR, but contains uncertainties of cosine error (COSERROR unit, k=2)
# type(s): uint(8), single, single ...
[UNCERTAINTY]
0       303.41  0       0       0       ...     0       0       0
1       306.75  17.92   17.92   15.41   ...     13.25   31.95   31.95
2       310.09  17.66   17.66   8.4     ...     10.9    14.65   14.65
...
253     1130.55 1479.92 1479.92 389.57  ...     530.24  1110.7  1110.7
254     1133.63 982.55  982.55  501.34  ...     497.42  851.74  851.74
255     1136.7  881.37  881.37  327.85  ...     385.86  752.05  752.05
[END_OF_UNCERTAINTY]

[AZIMUTH_ANGLE]
# type(s): single
90,0

# header row of the following table, containing incident angles (deg)
# type(s): string, string, single ...
px      wl\angle       -90     -85     -80     ...     80      85      90

# deviation from cosine law (%)
# type(s): uint(8), single, single ...
[COSERROR]
0       303.41  3       3       3       ...     3       3       3
1       306.75  9.48    9.48    -3.23   ...     -3.21   11.39   11.39
```

```
2       310.09  6.05    6.05    -3.71   ...     -3.35   14.4    14.4
...
253     1130.55 13.93   13.93   -38.48  ...     40.55   236.03  236.03
254     1133.63 -8.62   -8.62   28.93   ...     -63.57  -74.16  -74.16
255     1136.7  313.88  313.88  198.37  ...     175.01  241.13  241.13
[END_OF_COSERROR]

# header row of the following table, containing incident angles (deg)
# type(s): string, string, single ...
[COLUMN_NAMES]
px      wl\angle        -90     -85     -80     ...     80      85      90

# the same as COSERROR, but contains uncertainties of cosine error (COSERROR unit, k=2)
# type(s): uint(8), single, single ...
[UNCERTAINTY]
0       303.41  0       0       0       ...     0       0       0
1       306.75  27.13   27.13   11.75   ...     14.64   26.79   26.79
2       310.09  22.81   22.81   6.49    ...     8.16    12.82   12.82
...
253     1130.55 1240.34 1240.34 551.24  ...     488.5   1157.3  1157.3
254     1133.63 1065.09 1065.09 408.4   ...     556.71  994.89  994.89
255     1136.7  955.37  955.37  369.23  ...     428.03  773.2   773.2
[END_OF_UNCERTAINTY]
```

A3 Polarization sensitivity characterisation files

```
!FRM4SOC_CP
!POLDATA
# polarization sensitivity characterization results

# comments start with # (ignored by the processor)
# no empty lines between the parameter signatures in [] and the parameter values
# parameters are case insensitive
# parameters can be inserted in any order, except the first two signatures
# columns are tab- or space-delimited

# file format version
# type(s): string(255)
[VERSION]
0.1

# calibration date yyyy-mm-dd hh:mm:ss
# type(s): string(255)
[CALDATE]
2025-09-02 12:20:25

# calibration lab name
# type(s): string(255)
[CALLAB]
Tartu Observatory

# calibration lab person to contact
# type(s): string(255)
[USER]
Riho Vendt

# serial number of the calibrated instrument
# type(s): string(255)
# SAM_XXXX: TriOS Ramses, XXXX = Serial number
# SATXXXX: SeaBird/Satlantic HyperOCR, XXXX = Serial number
# DAL_XXXX_YYYYYY: IMO DALEC, XXXX = Serial number, YYYYYY = Module number
# e.g. SAM_8166, SAT0222, DAL_0012_144461
[DEVICE]
SAT2073
```

```
# lab temperature (deg Celsius) during cal/char measurements
# type(s): single
[AMBIENT_TEMP]
21.0

# radiometer internal temperature (deg Celsius) during cal/char measurements when available
# optional
# type(s): single
[DEVICE_TEMP]
23.88

# pixel no, wavelength (nm), semi-amplitude, uncertainty (k=2), angle of the max sensitivity
plane (rad), uncertainty (rad, k=2)
# type(s): uint8, single, single, single, single, single
[CALDATA]
0       306.36  0.00E+00        0.00E+00        0.00E+00        0.00E+00
1       309.69  3.77E-02        2.78E-02        2.61E+02        4.34E+01
2       313.03  4.26E-02        2.56E-02        2.63E+02        3.51E+01
...
253     1138.95 3.41E-02        1.08E-01        3.19E+02        3.41E+02
254     1142.07 2.26E-01        1.34E-01        2.38E+02        4.54E+01
255     1145.18 7.27E-02        9.61E-02        1.26E+02        1.08E+02
[END_OF_CALDATA]
```

A4 Straylight characterisation files

```
!FRM4SOC_CP
!STRAYDATA
# straylight characterization results

# comments start with # (ignored by the processor)
# no empty lines between the parameter signatures in [] and the parameter values

# parameters are case insensitive
# parameters can be inserted in any order, except the first two signatures

# columns are tab- or space-delimited

# file format version
# type(s): string(255)
[VERSION]
0.1

# calibration date yyyy-mm-dd hh:mm:ss
# type(s): string(255)
[CALDATE]
2025-09-02 12:20:25

# calibration lab name
# type(s): string(255)
[CALLAB]
Tartu Observatory

# calibration lab person to contact
# type(s): string(255)
[USER]
Riho Vendt

# serial number of the calibrated instrument
# type(s): string(255)
# SAM_XXXX: TriOS Ramses, XXXX = Serial number
# SATXXXX: SeaBird/Satlantic HyperOCR, XXXX = Serial number
# DAL_XXXX_YYYYYY: IMO DALEC, XXXX = Serial number, YYYYYY = Module number
# e.g. SAM_8166, SAT0222, DAL_0012_144461
[DEVICE]
```

```
SAT2073

# lab temperature (deg Celsius) during cal/char measurements
# type(s): single
[AMBIENT_TEMP]
21.0

# radiometer internal temperature (deg Celsius) during cal/char measurements when available
# optional
# type(s): single
[DEVICE_TEMP]
23.88

# n x n matrix, n depends on the device family (for RAMSES, HyperOCR & DALEC n=256)
# type(s): single, single ...
[LSF]
1.00E+00        0.00E+00        0.00E+00        ...     0.00E+00        0.00E+00        0.000E+00c
0.00E+00        1.00E+00        6.30E-01        ...     0.00E+00        0.00E+00        0.00E+00
0.00E+00        0.00E+00        1.00E+00        ...     0.00E+00        0.00E+00        0.00E+00
...
0.00E+00        0.00E+00        -7.42E-06       ...     1.00E+00        0.00E+00        0.00E+00
0.00E+00        0.00E+00        -7.67E-06       ...     0.00E+00        1.00E+00        0.00E+00
0.00E+00        0.00E+00        -6.64E-05       ...     0.00E+00        0.00E+00        1.00E+00
[END_OF_LSF]

#standard deviation of the previous table
# type(s): single, single ...
[UNCERTAINTY]
0.00E+00        0.00E+00        0.00E+00        ...     0.00E+00        0.00E+00        0.00E+00
0.00E+00        0.00E+00        8.56E-04        ...     0.00E+00        0.00E+00        0.00E+00
0.00E+00        0.00E+00        0.00E+00        ...     0.00E+00        0.00E+00        0.00E+00
...
0.00E+00        0.00E+00        1.55E-06        ...     0.00E+00        0.00E+00        0.00E+00
0.00E+00        0.00E+00        1.50E-06        ...     0.00E+00        0.00E+00        0.00E+00
0.00E+00        0.00E+00        2.72E-06        ...     0.00E+00        0.00E+00        0.00E+00
[END_OF_UNCERTAINTY]
```

A5 Thermal characterisation files

```
!FRM4SOC_CP
!TEMPDATA
# thermal characterization results

# comments start with # (ignored by the processor)
# no empty lines between the parameter signatures in [] and the parameter values
# parameters are case insensitive
# parameters can be inserted in any order, except the first two signatures
# columns are tab- or space-delimited

# file format version
# type(s): string(255)
[VERSION]
0.1

# calibration date yyyy-mm-dd hh:mm:ss
# type(s): string(255)
[CALDATE]
2025-09-02 12:20:25

# calibration lab name
# type(s): string(255)
[CALLAB]
Tartu Observatory

# calibration lab person to contact
```

```
# type(s): string(255)
[USER]
Riho Vendt

# serial number of the calibrated instrument
# type(s): string(255)
# SAM_XXXX: TriOS Ramses, XXXX = Serial number
# SATXXXX: SeaBird/Satlantic HyperOCR, XXXX = Serial number
# DAL_XXXX_YYYYYY: IMO DALEC, XXXX = Serial number, YYYYYY = Module number
# e.g. SAM_8166, SAT0222, DAL_0012_144461
[DEVICE]
SAT2073

# lab temperature (deg Celsius) during cal/char measurements
# type(s): single
[AMBIENT_TEMP]
21.0

# radiometer internal temperature (deg Celsius) during cal/char measurements when available
# optional
# type(s): single
[DEVICE_TEMP]
23.88

# pixel no, thermal coefficient (1/deg), uncertainty (1/deg, k=2)
# type(s): uint8, single, single, single
[CALDATA]
0       303.01  8.659E-006     2.050E-004
1       306.32  2.521E-004     2.672E-003
2       309.64  1.458E-003     2.224E-003
...
253     1136.07 9.507E-003     9.936E-002
254     1139.21 -4.601E-002    1.423E-001
255     1142.35 -2.752E-002    1.243E-001
[END_OF_CALDATA]
```

Annex B. The calibration process: A Step-by-Step Guide

B1 Preparing for the lab environment.

Ensure that all the equipment needed for calibration is in good working condition and calibrated. Valid calibration is critical for calibration sources (lamps, panels, spheres), radiometric power supplies and distance tools. Calibration of environmental sensors is strongly recommended. Install the optical tables, rails, baffles etc. and remove the irrelevant equipment if possible.

B2 Receiving the radiometers.

The receiving process depends on the lab's established practices, but documenting the steps is strongly advised. Inspect the containers for possible damage. After opening the containers, visually inspect the content. Report all possible issues back to the customer before proceeding. Create the list of items (radiometers, protection caps, cables etc.) to avoid confusion later. Ensure that the radiometers have distinctive serial numbers and that the numbers coincide with the ones in the order.

B3 Testing the connections & software.

Test the radiometer's functionality before going to the lab. Ensure that all necessary cables, power supplies, connection boxes etc. are present and functioning. Get familiar with the controlling software, install factory files when needed and ensure the basic functionality by acquiring light and dark sample spectra.

B4 Cleaning the radiometers.

The radiometers can be severely fouled when arriving from the field work and some overall cleaning is needed to protect the lab against contamination. The cables, power supplies, and other accessories need cleaning as well. As in general, the input optics need to be clean to maintain a consistent calibration baseline. De-ionized water and optics-grade wipes are sufficient and safe in most cases. Consult with the manufacturers before using any organic solvents. In some cases, users might be interested in the "dirty" (post-deployment) calibration, followed by the "clean" (pre-deployment) calibration. Then, it is advisable to clean the input optics directly in the calibration setup to avoid systematic effects due to the re-alignment and source drift. The input optics must be completely dry before the calibration measurements. The calibration source shall be protected against sprinkle liquids and strong air flows during the sensor cleaning and drying.

The connectors need attention as well. The Subconn connectors, for example, need lubrication (instructions from the manufacturer's webpage). Avoid contamination of the optical surfaces with the lubricant.

B5 Set-up and alignment.

Typical setups for the absolute spectral irradiance and radiance calibrations are shown in *Figure 6-1*, *Figure 6-2* and *Figure 6-3* of this document. The alignment sequence for spectral radiance in Tartu Observatory is as follows:

Level the optical rail when needed; install adapters for the lamp, the radiometer, the panel and any auxiliary equipment (stability monitor, temperature sensor etc.).

Install the dual-beam laser and set up the main optical axis.

Install the FEL lamp and connect the cables.

Install the alignment jig to the lamp.

Adjust the lamp holder to get the reflection from the central target of the jig back to the dual-beam laser front window.

Remove the alignment jig.

Attach the mirror jig to the panel adapter.

Adjust the panel adapter so that the laser spot hits the center of the jig mirror, perpendicular to the optical axis.

Remove the dual-beam laser.

Install the distance probe and set the distance of 500 mm between the lamp and the mirror jig.

Install the dual-beam laser.

Rotate the mirror jig in the panel adapter to get the displaced by 45° laser beam.

Install the radiance sensor to be calibrated so that the laser beam hits the center of it's input aperture.

Place the environmental sensor close to the front end of the radiometer.

Align the radiance sensor to get the reflection of the laser beam back to the laser output window.

Remove the dual-beam laser.

Remove the mirror jig from the panel adapter and install the reflectance panel.

Place the distance probe between the lamp and the panel and set the 500 mm distance.

Remove the distance probe

The alignment steps should be repeated until no visible misalignment can be detected.

B6 Before the calibration.

Ensure proper functioning of the radiometer to be calibrated.

Ensure proper functioning of the calibration and auxiliary devices (power supply, shutter, monitors, temperature sensors etc.).

Write down the serial numbers of the calibration and auxiliary equipment.

Check the lamp polarity, serial number and voltage settings of the power supply.

Ensure the calibration source is cleared to switch on (remove protective covers, alignment equipment etc.).

Switch on the calibration source, adjust the power according to the instructions and wait for stabilization at least 20 minutes before the calibration measurements.

B7 During the calibration.

(If not automated:) Log the operations manually (datetime, serial numbers, gains, integration times, shutter operation, measurement sequence, number of repeats etc.).

As in the case with the TriOS RAMSES, Sea-Bird HyperOCR and *In-situ* Marine Optics DALEC, it is recommended to take measurements with at least two integration times: one auto-probed (the longest integration time avoiding over-exposure) and the second one twice shorter. Averaging of 20 to 40 spectra is sufficient.

Dark (or background) should be measured with the same integration times and timely close to the light measurements.

Control that the recorded data files contain all valid information as needed.

If pre- and post-deployment calibrations are required, clean the input optics of the radiometer without removing the radiometer and repeat the calibration measurements. Avoid damaging the calibration source by cleaning agent or compressed air.

B8 After the calibration.

Switch off the calibration source according to the instructions. Don't perform any operations with the lamp for 20 minutes of cooling.

Log the source's burning time.

Switch off auxiliary devices.

If applicable, do not dismantle the set-up before the final data processing as re-check of the geometry or repeated calibration might be needed.

Process the collected data by calculating the calibration coefficients with uncertainties.

Contact the customer regarding any unexpected findings.

Format the output as necessary, e.g. the device files, HyperCP files or spreadsheet.

Back up the measured data, calculation method and output files.

Recheck the radiometers for possible damage.

Pack the radiometers according to the list created earlier. If required, include copies of the certificates, data etc.